From Boundary Data to Bound States III: Radiative Effects

G. Cho, G. Kälin, R. A. Porto

Deutsches Elektronen-Synchrotron DESY, Hamburg

Herausgeber und Vertrieb:

Verlag Deutsches Elektronen-Synchrotron DESY

DESY Bibliothek
Notkestr. 85
22607 Hamburg
Germany

arXiv:2112.03976v2 [hep-th] 27 May 2022

From Boundary Data to Bound States III:
Radiative Effects

Gihyuk Cho, Gregor Kälin and Rafael A. Porto

Deutsches Elektronen-Synchrotron DESY, Notkestr. 85, 22607 Hamburg, Germany

E-mail: gihyuk.cho@desy.de, gregor.kaelin@desy.de, rafael.porto@desy.de

ABSTRACT: We extend the *boundary-to-bound* (B2B) correspondence to incorporate radiative as well as conservative radiation-reaction effects. We start by deriving a map between the total change in observables due to gravitational wave emission during hyperbolic-like motion and in one period of an elliptic-like orbit, which is valid in the adiabatic expansion for non-spinning as well as aligned-spin configurations. We also discuss the inverse problem of extracting the associated fluxes from scattering data. Afterwards we demonstrate, to all orders in the Post-Minkowskian expansion, the link between the radiated energy and the ultraviolet pole in the radial action in dimensional regularization due to tail effects. This implies, as expected, that the B2B correspondence for the conservative sector remains unchanged for local-in-time radiation-reaction tail effects with generic orbits. As a side product, this allows us to read off the energy flux from the associated pole in the tail Hamiltonian. We show that the B2B map also holds for non-local-in-time terms, but only in the *large-eccentricity* limit. Remarkably, we find that all of the trademark logarithmic contributions to the radial action map unscathed between generic unbound and bound motion. However, unlike logarithms, other terms due to non-local effects do not transition smoothly to *quasi-circular* orbits. We conclude with a discussion on these non-local pieces. Several checks of the B2B dictionary are displayed using state-of-the-art knowledge in Post-Newtonian/Minkowskian theory.

Contents

1 Introduction

Motivated by the 'on-shell' nature of scattering processes, a *boundary-to-bound* (B2B) correspondence between observables, such as the deflection angle and periastron advance, was introduced in [1, 2] for the (strictly) conservative sector. The B2B map connects hyperbolic-to elliptic-like orbits through analytic continuation of the radial action without resorting to gauge-dependent objects like the Hamiltonian. With the goal of using Post-Minkowskian (PM) scattering data — obtained through (quantum) amplitude-based, e.g. [3–18], and (classical) EFT-based, e.g. [19–33], methodologies — to construct high-precision Post-Newtonian (PN) waveform models, e.g. [34], the purpose of this paper is to extend the B2B dictionary to the radiation sector. Radiative effects in the two-body dynamics come in two flavors. Firstly, there is the obvious loss of energy and angular momentum due to gravitational wave (GW) emission responsible for the celebrated change in the orbital parameters. There are, however, also 'conservative' radiation-reaction contributions to, for instance, the binding energy. These arise due to non-linear gravitational effects, such as the GWs getting trapped in the near zone through scattering off of the background geometry, so-called *tail* effects, see e.g. [35, 36], or off of the waves emitted at an earlier time, so-called the (non-linear) *memory*.[1] We study here the B2B map for both dissipative and conservative radiation-reaction effects.

In principle, the instantaneous dynamics due to dissipation produces various transient phenomena associated with radiation-reaction forces which cannot be captured by the conservative equations of motion, e.g. [37–39]. However, provided the adiabatic expansion holds, we can evaluate the total loss of energy and angular momentum by integrating the (averaged) instantaneous flux using the unperturbed (conservative) solution. Here is where the original B2B dictionary [1, 2] — linking the point of closest approach in a scattering process to the endpoints of elliptic-like orbits via analytic continuation in the angular momentum and binding energy — becomes extremely powerful. After taking into account the parity properties under $J \to -J$ of the associated fluxes, we show the following relationships,

$$\Delta E_{\mathrm{ell}}(J) = \Delta E_{\mathrm{hyp}}(J) - \Delta E_{\mathrm{hyp}}(-J), \qquad \Delta J_{\mathrm{ell}}(J) = \Delta J_{\mathrm{hyp}}(J) + \Delta J_{\mathrm{hyp}}(-J),$$

hold between the total radiated (source) energy and angular momentum in a scattering process and one orbit of elliptic-like motion, valid for non-spinning or aligned-spin configurations. As we shall see, the analytic continuation also holds in terms of the eccentricity parameter, which will be useful when performing the B2B map between radiative observables.

Although the above relations already uncover a non-trivial link between radiation effects for unbound and bound states, to compute the GW phase for generic orbits requires the (averaged) instantaneous flux. From the point of view of scattering, the inverse problem then turns into obtaining the flux from the knowledge of the total radiated energy. Following similar steps as for the Firsov representation discussed in [1, 2], we show here how to reconstruct the GW flux in an isotropic gauge from the PM expansion of the radiated energy.

---

[1]We will concentrate mostly on tail terms in this paper. We briefly discuss memory corrections in §6.

In order to complete all the necessary ingredients for accurate waveform modeling we must also incorporate conservative corrections due to hereditary effects. As it turns out, these come in different forms since not only they introduce the standard local-in-time interactions, but are also responsible for non-local-in-time effects [35]. The latter are a trademark of tail-type contributions and do not appear with memory terms. In combination with the existence of spurious infrared/ultraviolet divergences in intermediate computations from the near (potential) and far (radiation) zones, the time non-locality induces a breakdown of the near/far zone expansion that caused the introduction of several (apparent) *ambiguities* in 'traditional' PN computations [40–45]. These issues, however, are naturally handled within the EFT approach [46–51], resulting in completely unambiguous answers [52–55]. Yet, because of a variety of contributions and mixing between zones, the EFT split into potential and radiation modes can be further decomposed into (generalized) local- and non-local-in-time effects. The latter separation, which we adopt in this paper, is advantageous when it comes to applying the B2B dictionary as well as incorporating the true logarithmic corrections to the binary dynamics.

In order to establish the extension of the B2B correspondence, we start by demonstrating the universal connection between the energy flux, $\mathcal{F}_E$, and the ultraviolet-divergent part of the tail contribution to the Hamiltonian, H_{tail}, due to radiation modes [26, 27],

$$\frac{H_{\text{tail}}(r, \boldsymbol{p}^2)}{GE} = \frac{\mathcal{F}_E(r, \boldsymbol{p}^2)}{(d-4)_{\text{UV}}} + \cdots,$$

which cancels out against an infrared pole arising from the potential region [53]. From here, and the connection between the effective and radial actions, we conclude that the B2B dictionary remains valid for local-in-time effects. The fact that the latter can be mapped from unbound to bound motion through the original B2B dictionary is not surprising. After all, if we shuffle all of the logarithms into the non-local part the remaining pieces can be parameterized using the standard PM expansion for the center-of-mass momentum which, using the manipulations in [1, 2], yield the original B2B relations. What is instructive, however, is to notice that, due to the universal connection between the flux and the tail Hamiltonian, or likewise the radiated energy and radial action, the B2B correspondence in the dissipative sector is intimately linked to the B2B map for conservative local-in-time effects.

The situation changes dramatically for non-local-in time terms. While we can, once again, resort to an adiabatic expansion in which the hereditary integral is computed over the conservative motion, the resulting dynamical equations vary significantly between hyperbolic-like motion and generic bound orbits. Nonetheless, we find that the original B2B correspondence applies [1, 2]

$$\mathcal{S}_{r,\text{ell}}(J) = \mathcal{S}_{r,\text{hyp}}(J) - \mathcal{S}_{r,\text{hyp}}(-J),$$

for the full radial action, but only in the limit of large angular momentum, also known as the *large-eccentricity* limit.

Unfortunately, the resulting coefficients in the $1/J$ expansion do not capture generic terms associated with non-local-in-time effects for e.g. quasi-circular motion. Nevertheless, not only can we map all of the local-in-time contributions in this fashion, remarkably the large-eccentricity limit readily accounts for all the leading logarithmic corrections in $\mathcal{E}$, the (reduced) binding energy, which take on the universal form

$$\mathcal{S}^{\log}_{r,\text{hyp/ell}} = -\frac{GE}{2\pi} \Delta E_{\text{hyp/ell}} \log |\mathcal{E}| \, ,$$

and may be obtained through the original B2B (bound) radial action via the scattering angle [1, 2]. Moreover, we also find the center-of-mass momentum can be reconstructed in terms of an (effectively local) PM expansion in G/r, which correctly incorporates both local-in-time as well as non-local-in-time effects proportional to logarithms of the binding energy. In combination with Firsov's representation, this allows us to read off all of the associated coefficients in the $1/J$ expansion of the radial action to a given PN order [1, 2]. At the same time, it illustrates how — unlike the intermediate potential-only results — the spurious factors of $\log r$ in the center-of-mass momentum [26] or Hamiltonian [14] do not appear in the complete (ambiguity-free) dynamics [27].

After demonstrating the existence of an extended B2B correspondence in the radiative sector,[2] we dedicate the penultimate section to various explicit checks of the B2B map using the state-of-the-art in the PN/PM expansion both for non-spinning and aligned-spin configurations. To the extent of our knowledge, the computations of the total radiated energy and angular momentum including spin effects using the fluxes obtained in [57] — which we display here in their full glory — are presented for the first time. While our results for the conservative sector are completely generic, we restrict ourselves to the well understood local- and non-local-in-time contributions at 4PN order derived through different methodologies in [42–45, 52–55], except for logarithmic terms which we incorporate to 6PN order using the results in [58]. In addition, we have explicitly checked the B2B map applies to the contributions at 5PN reported in [59] as well as the intermediate results in [60]. We will make a few comments at the end regarding conservative (local-in-time) memory terms.

The final section of this paper is devoted to a discussion on plausible ways to map generic non-local-in-time effects from scattering processes to generic bound states. Throughout this paper we follow the conventions and notation of [1, 2], to which we refer to reader for further details. We also provide an ancillary file collecting the main expressions presented here.

---

[2]An intriguing connection resembling the B2B map was recently discussed in [56]. It would be interesting to explore whether it also extends to the radiative sector.

2 Orbital elements

One of the key ideas behind the B2B dictionary is the link between the endpoints of elliptic-like motion and closest approach in hyperbolic encounters, see Fig. 1. Here we summarize the correspondence and add also a few additional elements which play an important role later on when performing the analytic continuation between unbound and bound motion.

2.1 $J \to -J$

In the original B2B map in [1, 2] for observables in the conservative sector, the endpoints of a bound orbit, $0 < r_- < r_+$, were shown to be related to the distance of closest approach in a scattering event, $\tilde{r}_-$, via analytic continuation,

$$r_-(J, \mathcal{E}) = \tilde{r}_-(J, \mathcal{E}), \tag{2.1}$$
$$r_+(J, \mathcal{E}) = \tilde{r}_-(-J, \mathcal{E}),$$

with positive (total) angular momentum, $J > 0$, and negative binding energy, $\mathcal{E} \equiv \frac{E-M}{M\nu} < 0$, respectively, where $M = m_1 + m_2$ is the total mass, E the total energy, and ν the symmetric-mass-ratio. The above relationships are a direct consequence of Firsov's representation for the momentum of the incoming particles in the center-of-mass frame, [61]

$$\bar{\boldsymbol{p}}^2 = \exp\left[\frac{2}{\pi} \int_{r|\bar{\boldsymbol{p}}|}^{\infty} \frac{\chi(\tilde{b}_c) \mathrm{d}\tilde{b}_c}{\sqrt{\tilde{b}_c^2 - r^2 \bar{\boldsymbol{p}}^2}}\right] = 1 + \sum_{i=1}^{\infty} f_i(\mathcal{E}, L, a_\pm) \left(\frac{GM}{r}\right)^i, \tag{2.2}$$

where $\bar{\boldsymbol{p}}^2 \equiv \boldsymbol{p}^2/p_\infty^2$ with p_∞ the incoming momentum at infinity, $\chi(\tilde{b}_c)$ is the scattering angle, $a_\pm = a_1 \pm a_2$ with a_i the (mass-rescaled) spin parameters, and $b_c \equiv L/p_\infty$. The (canonical) orbital angular momentum, L, obeys the relation [62]

$$L = p_\infty b + M \frac{\Gamma - 1}{2} \left(a_+ - \frac{\Delta}{\Gamma} a_-\right), \tag{2.3}$$

with b the (covariant) impact parameter. We have also introduced the notation $\Gamma \equiv E/M$, $\Delta \equiv \sqrt{1 - 4\nu}$. From here we obtain

$$\tilde{r}_- = b_c \exp\left[-\frac{1}{\pi} \int_{b_c}^{\infty} \frac{\chi(\tilde{b}_c) \mathrm{d}\tilde{b}_c}{\sqrt{\tilde{b}_c^2 - b_c^2}}\right], \tag{2.4}$$

for the (real and positive) root of the vanishing radial momentum at the point of closest proximity,

$$\bar{p}_r^2(\tilde{r}_-) = \bar{\boldsymbol{p}}^2(\tilde{r}_-) - b_c^2/\tilde{r}_-^2 = 0. \tag{2.5}$$

It is straightforward to show a relationship similar to the one implied by (2.1) also applies for the other (unphysical) root, $\tilde{r}_+ < 0$, of the unbound motion; namely

$$\tilde{r}_+(J, \mathcal{E}) = \tilde{r}_-(-J, \mathcal{E}), \tag{2.6}$$

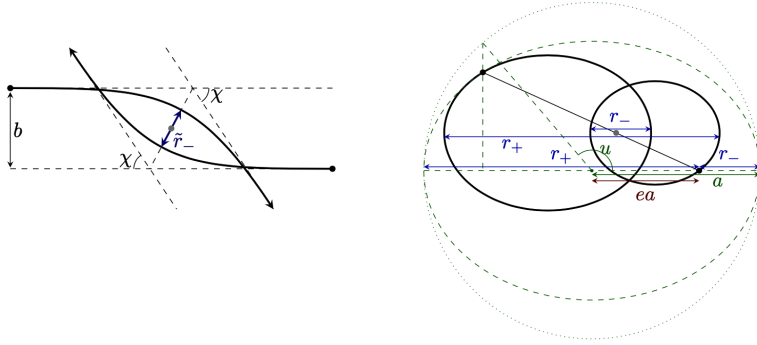from positive (total) angular momentum $J > 0$, but this time having both positive binding energy, $\mathcal{E} > 0$.

Figure 1: The geometry for unbound and bound motion. See the text for definition of the various variables.

2.2 $e \to -e$

From the roots of the radial momentum we can construct the parameters describing the eccentricity of the orbit,

$$
\begin{aligned}
e &= \frac{r_+ - r_-}{r_+ + r_-} \qquad \text{(ellipse)}, \\
\tilde{e} &= \frac{\tilde{r}_+ - \tilde{r}_-}{\tilde{r}_+ + \tilde{r}_-} \qquad \text{(hyperbola)}.
\end{aligned}
\tag{2.7}
$$

From the conditions in (2.1) and (2.6) we notice that $J \to -J$ implies $e \to -e$, and similarly $\tilde{e} \to -\tilde{e}$. This means, for instance, the B2B relationship between scattering angle and periastron advance [2]

$$
\Delta\Phi(J, \mathcal{E}) = \chi(J, \mathcal{E}) + \chi(-J, \mathcal{E}),
\tag{2.8}
$$

may also be written as

$$
\Delta\Phi(e, \mathcal{E}) = \chi(e, \mathcal{E}) + \chi(-e, \mathcal{E}),
\tag{2.9}
$$

analytically continued to $e < 1$ and negative binding energies.[3] The map involving eccentricities will prove to be useful when studying radiative observables next.

3 Radiative observables

In this section we focus on the total change induced on observables due to GW radiation in a scattering process and one period of elliptic-like motion. In all cases we will assume the validity of the adiabatic expansion; namely, that we can evaluate the total change by integrating the (averaged) fluxes over the solution of the conservative dynamical equations. This will allow us to use the connection between the orbital elements described above. Moreover, we will concentrate here either on non-spinning or aligned-spin configurations, such that motion remains in a plane orthogonal to the total angular momentum.

---

[3]We thank M. van de Meent for demonstrating the exact validity of (2.8)-(2.9) for the case of a test body in a Schwarzschild background (unpublished).

3.1 J-parity

Let us consider the (averaged) flux, $\mathcal{F}_\mathcal{O}(r, \mathcal{E}, L, a_\pm)$, associated with an observable quantity. The total change may be then written as follows

$$
\begin{aligned}
\Delta\mathcal{O}_{\text{ell}} &= \int_0^{T_{\text{orb}}} \mathcal{F}_\mathcal{O}(r, \mathcal{E}, L, a_\pm) dt = 2\int_{r_-}^{r_+} \mathcal{F}_\mathcal{O}(r, \mathcal{E}, L, a_\pm)\frac{dr}{\dot{r}}\,, \\
\Delta\mathcal{O}_{\text{hyp}} &= \int_{-\infty}^{+\infty} \mathcal{F}_\mathcal{O}(r, \mathcal{E}, L, a_\pm) dt = 2\int_{\tilde{r}_-}^{\infty} \mathcal{F}_\mathcal{O}(r, \mathcal{E}, L, a_\pm)\frac{dr}{\dot{r}}\,,
\end{aligned}
\tag{3.1}
$$

for elliptic- and hyperbolic-like motion, respectively. Assuming the validity of an adiabatic approximation, and using the conservative equations of motion in a quasi-isotropic gauge[4]

$$
\dot{r} = 2\frac{\partial H}{\partial \boldsymbol{p}^2}\,p_r\,,
\tag{3.2}
$$

with H the Hamiltonian, as well as (see (2.2))

$$
p_r^2 = \boldsymbol{p}^2 - J^2/r^2\,,
\tag{3.3}
$$

we arrive at

$$
\begin{aligned}
\Delta\mathcal{O}_{\text{ell}} &= \int_{r_-}^{r_+} \left(\frac{\partial H}{\partial \boldsymbol{p}^2}\right)^{-1} \frac{\mathcal{F}_\mathcal{O}(r, \mathcal{E}, L, a_\pm)}{\sqrt{\boldsymbol{p}^2(r, \mathcal{E}, L, a_\pm) - J^2/r^2}} dr\,, \\
\Delta\mathcal{O}_{\text{hyp}} &= \int_{\tilde{r}_-}^{\infty} \left(\frac{\partial H}{\partial \boldsymbol{p}^2}\right)^{-1} \frac{\mathcal{F}_\mathcal{O}(r, \mathcal{E}, L, a_\pm)}{\sqrt{\boldsymbol{p}^2(r, \mathcal{E}, L, a_\pm) - J^2/r^2}} dr\,.
\end{aligned}
\tag{3.4}
$$

Since the Hamiltonian is a function of r, $\boldsymbol{p}^2$, $a_\pm^2$, and $La_\pm$, the extension of the B2B dictionary hinges upon the properties under a "J-parity" transformation: $L \to -L$ and $a_\pm \to -a_\pm$, of the given fluxes

$$
\mathcal{F}_\mathcal{O}(r, \mathcal{E}, -J) = \sigma_\mathcal{O}\,\mathcal{F}_\mathcal{O}(r, \mathcal{E}, J)\,,
\tag{3.5}
$$

with $\sigma_\mathcal{O} = \pm 1$. By performing the same *loop around infinity* as in (2.8), we find

$$
\Delta\mathcal{O}_{\text{ell}}(J, \mathcal{E}) = \Delta\mathcal{O}_{\text{hyp}}(J, \mathcal{E}) - \sigma_\mathcal{O}\Delta\mathcal{O}_{\text{hyp}}(-J, \mathcal{E})\,,
\tag{3.6}
$$

which, as we discussed earlier, can also be written as

$$
\Delta\mathcal{O}_{\text{ell}}(e, \mathcal{E}) = \Delta\mathcal{O}_{\text{hyp}}(e, \mathcal{E}) - \sigma_\mathcal{O}\Delta\mathcal{O}_{\text{hyp}}(-e, \mathcal{E})\,.
\tag{3.7}
$$

These manipulations allow us to relate the total change for several observable quantities computed in unbound and bound orbits.

---

[4]In principle there is also a correction to $\dot{\boldsymbol{r}}$ proportional to $\boldsymbol{r} \times \frac{\partial H}{\partial \boldsymbol{L}}$. However, it does not contribute to $\dot{r}$.

3.2 Energy

The case of the total radiated energy is the simplest. Firstly, we notice that in an quasi-isotropic gauge we have

$$\mathcal{F}_E(r, \mathcal{E}, -J) = +\mathcal{F}_E(r, \mathcal{E}, J),\tag{3.8}$$

for the energy flux, almost trivially since it can be written as a function of r, $\boldsymbol{p}^2$, $a_\pm^2$ and $La_\pm$.[5] This is not surprising since we expect the flux to be a scalar under J-parity. Following our previous reasoning we then arrive at [26]

$$\begin{aligned}
\Delta E_{\text{ell}}(J, \mathcal{E}) &= \Delta E_{\text{hyp}}(J, \mathcal{E}) - \Delta E_{\text{hyp}}(-J, \mathcal{E}),\\
\Delta E_{\text{ell}}(e, \mathcal{E}) &= \Delta E_{\text{hyp}}(e, \mathcal{E}) - \Delta E_{\text{hyp}}(-e, \mathcal{E}),
\end{aligned}\tag{3.9}$$

which was previously observed to hold in [58] (for the $J \to -J$ map) with the knowledge of the PN expansion at the time. We show here that, as expected, it continues to hold for the recently derived results at 3PN order [63].

3.3 Angular momentum

We can also apply the map to the angular momentum. Being a pseudo-vector, its flux must transform under J-parity in the same fashion as the angular momentum itself,

$$\mathcal{F}_J(r, \mathcal{E}, -J) = -\mathcal{F}_J(r, \mathcal{E}, J).\tag{3.10}$$

Therefore, the correspondence between elliptic- and hyperbolic-like motion becomes

$$\begin{aligned}
\Delta J_{\text{ell}}(J, \mathcal{E}) &= \Delta J_{\text{hyp}}(J, \mathcal{E}) + \Delta J_{\text{hyp}}(-J, \mathcal{E}),\\
\Delta J_{\text{ell}}(e, \mathcal{E}) &= \Delta J_{\text{hyp}}(e, \mathcal{E}) + \Delta J_{\text{hyp}}(-e, \mathcal{E}),
\end{aligned}\tag{3.11}$$

similarly to that of the periastron advance and scattering angle.

3.4 Inverse problem

For the conservative sector, the Firsov representation in (2.2) allows us to construct a (gauge-dependent) object to describe the dynamics from the knowledge of the scattering angle. The main idea is to invert the integral which defines the latter in terms of the radial momentum. A similar representation can then be shown to exist for the GW flux in terms of the total radiated energy and angular momentum. For the sake of simplicity we consider the non-spinning case. Let us stare at the expressions for the total radiated energy,

$$\begin{aligned}
\Delta E_{\text{hyp}} &= \int_{\tilde{r}_-}^{\infty} \left(\frac{\partial H(r, \boldsymbol{p}^2)}{\partial \boldsymbol{p}^2}\right)^{-1} \frac{\mathcal{F}_E(r, \mathcal{E})}{\sqrt{\boldsymbol{p}^2(r, \mathcal{E}) - J^2/r^2}} dr\\
\Delta E_{\text{ell}} &= \int_{r_-}^{r^+} \left(\frac{\partial H(r, \boldsymbol{p}^2)}{\partial \boldsymbol{p}^2}\right)^{-1} \frac{\mathcal{F}_E(r, \mathcal{E})}{\sqrt{\boldsymbol{p}^2(r, \mathcal{E}) - J^2/r^2}} dr
\end{aligned}\tag{3.12}$$

---

[5]The existence of this gauge is also connected to the link between the tail Hamiltonian and energy flux.

Since we are only concerned about the source energy, the associated flux may be expanded in powers of GM/r,

$$\mathcal{F}_E(r,\mathcal{E}) = \frac{M}{r} \sum_{n=0}^{\infty} \mathcal{F}_E^{(n)}(\mathcal{E}) \left(\frac{GM}{r}\right)^{n+3},\qquad(3.13)$$

with $\mathcal{F}_{\mathcal{E}}^{(n)}(\mathcal{E})$ (dimensionless) functions of the binding energy, and we chose the starting point of the sum in hindsight of the leading PN effects. From here, and the fact that the PM expansion of the Hamiltonian (and its derivatives) can be obtained via scattering data [1–3], we arrive at an integral involving only the radial motion and some functions of the binding energy. By performing the integration and expanding in G/J we can then read off the $\mathcal{F}_{\mathcal{E}}^{(n)}(\mathcal{E})$ coefficients directly from the PM expansion of the total radiated energy

$$\Delta E_{\text{hyp}}(j,\mathcal{E}) = \sum_{n=0}^{\infty} \Delta E_{\text{hyp}}^{(n)}(\mathcal{E}) \frac{1}{j^{n+3}},$$
$$\Delta E_{\text{ell}}(j,\mathcal{E}) = \Delta E_{\text{hyp}}(j,\mathcal{E}) - \Delta E_{\text{hyp}}(-j,\mathcal{E}),\qquad(3.14)$$

with $j \equiv J/(GM^2\nu)$. The final expressions, however, are rather cumbersome and not particularly illuminating (see ancillary file). Here we quote only the first two orders, obtained using the known PM results for the conservative sector [22],

$$M\pi\xi\,\mathcal{F}_E^{(0)} = \frac{2\Gamma\nu\Delta E_{\text{hyp}}^{(0)}}{(\gamma^2-1)},$$
$$M\pi\xi\,\mathcal{F}_E^{(1)} = \frac{3\pi\Gamma^2\nu\Delta E_{\text{hyp}}^{(1)}}{4(\gamma^2-1)^{3/2}} - \frac{2\Delta E_{\text{hyp}}^{(0)}\nu^3}{(\gamma^2-1)^2\Gamma^6\xi^2}\left[(\gamma-1)^3\left(10\gamma^3-10\gamma^2-9\gamma+5\right)\nu^2 \right.\qquad(3.15)$$
$$\left. +4\left(5\gamma^5-8\gamma^4+\gamma^3+4\gamma^2-3\gamma+1\right)\nu+8\gamma^4-4\gamma^2-1\right],$$

with

$$\xi \equiv E_1 E_2/E^2,\quad E_a \equiv \sqrt{p_\infty^2+m_a^2},\quad p_\infty^2 = \frac{M\nu}{\Gamma}(\gamma^2-1),\quad \gamma \equiv 1+\mathcal{E}+\frac{\nu}{2}\mathcal{E}^2,\qquad(3.16)$$

and provide an explicit derivation at 3PM in §5. A similar reasoning applies to the angular momentum. As we shall see shortly, the coefficients in the PM expansion in (3.13) can be also read off from the imprint of radiation-reaction effects in the conservative dynamics.

4 Conservative radiation-reaction

As it is well known hereditary back-reaction effects contribute to the conservative regime of the dynamics, e.g. [36, 52]. In this section we discuss the extension of the B2B dictionary to conservative radiation-reaction effects.

$$= \quad \times \quad iGE\omega \left[-\frac{(\omega^2 + i0^+)}{\pi\mu^2} e^{\gamma_E} \right]^{(d-4)/2} \left(\frac{2}{d-4} + \cdots \right)$$

Figure 2: Universal ultraviolet structure of the hereditary effects (in the far zone) at leading order in the $GE\omega$ expansion. The wavy and (doubly) solid lines represent the gravitational field and binary system, respectively. The latter is described by the (near zone) stress-energy tensor $T^{\mu\nu}$. Only tail terms contribute to the (ultraviolet) divergence [36]. The ellipses contain finite terms in the $d \to 4$ limit. See [64] for more details.

4.1 Universality

As it was shown some time ago in [64], the tail correction to the GW amplitude becomes

$$|\mathcal{A}_{\rm src} + \mathcal{A}_{\rm tail}|^2 = (1 + 2\pi GE\omega)|\mathcal{A}_{\rm src}|^2 + \mathcal{O}\left((GE\omega)^2\right) , \tag{4.1}$$

at leading order in the $(GE\omega)$ expansion in the far zone. The (source) amplitude, $\mathcal{A}_{\rm src}$, defined by

$$i\mathcal{A}_{\rm src}(\omega, \boldsymbol{k}) = -\frac{i}{2}\epsilon_{ij}^{\star}(\boldsymbol{k})T^{ij}(\omega, \boldsymbol{k}) , \tag{4.2}$$

depends upon the near-zone pseudo stress-energy tensor (including also the binding potential modes), $T^{ij}(\omega, \boldsymbol{k})$, as well as the polarization tensor, $\epsilon_{ij}(\boldsymbol{k})$. The above relation is a consequence of the link depicted in Fig. 2.[6]

At the same time we have a conservative contribution to the effective action, $S_{\rm eff}^{\rm tail} \equiv -\frac{1}{2\pi}\int_{-\infty}^{+\infty} H_{\rm tail}dt$, with $H_{\rm tail}$ the tail Hamiltonian, shown in Fig. 3. As discussed in [52, 65], the main difference between retarded and Feynman propagators involves the choice of $i0^+$ prescription, yielding a result with a left-over integral over $d\omega$ involving either

$$\begin{aligned}
\frac{1}{(d-4)} \left(\sqrt{-(\omega^2 + i0^+)} \right)^{(d-4)} &\quad \text{(Feynman)}, \quad \text{or} \\
\frac{1}{(d-4)} \left(\sqrt{-(\omega + i0^+)^2} \right)^{(d-4)} &\quad \text{(Retarded)},
\end{aligned} \tag{4.3}$$

in dimensional regularization in d dimensions. It is straightforward to show that the difference in the derivation in either case only affects the imaginary (dissipative) part. Indeed, the associated factor of $i\pi$ (versus $i\pi \, \text{sign}\,\omega$) is required from the optical theorem,

$$\text{Im Fig 3} = \frac{1}{2}\int \frac{d\Gamma_{\rm tail}}{d\omega}d\omega \quad \text{(Feynman)}, \tag{4.4}$$

---

[6]This is sometimes written in terms of so-called "radiative" multipole moments associated with the (long-wavelength) expansion of $T^{ij}(\omega, \boldsymbol{k})$ in powers of $\boldsymbol{k}$.
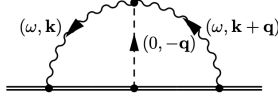
Figure 3: Correction to the effective action due to the leading tail effect. The wavy line is the (on-shell) radiation mode while the background geometry is sourced by the total energy represented by the dashed line. The causal routing features retarded propagators, see [52] for more details.

in order to match the integrated rate of graviton emission, Γ_{tail}, due to the tail effect. At the same time, after multiplying by the phase space measure on both sides of (4.1), we find

$$\frac{d\Gamma_{\text{tail}}}{d\omega} = 2\pi G E \frac{dE_{\text{src}}}{d\omega} + \mathcal{O}(GE\omega)^2)\,, \tag{4.5}$$

where $\omega d\Gamma_{\text{src}}/d\omega \equiv dE_{\text{src}}/d\omega$ is the source energy spectrum. This implies,

$$\text{Im Fig}\,3 = GE\pi \int \frac{dE_{\text{src}}}{d\omega} d\omega \qquad \text{(Feynman)}\,. \tag{4.6}$$

Since the factor of $i\pi$ is intimately connected to the ultraviolet pole (as well as logarithmic correction) in the real part of the effective action, whose residue is unaffected by the choice of propagators, we conclude the leading conservative contribution from the tail effect to the effective action must take on the following universal form:

$$\text{Fig}\,3 = -GE \int \frac{dE_{\text{src}}}{d\omega} \left(\frac{1}{(d-4)_{\text{UV}}} + \log\frac{\omega^2}{\mu^2} - i\pi\text{sign}\,\omega + \cdots\right) d\omega \qquad \text{(Retarded)}\,. \tag{4.7}$$

Notice that, while we work at leading order in the tail expansion in the radiation region, the expression in (4.7) enters at all PM orders due to $\mathcal{O}(G_N)$ corrections from the near zone to the source energy flux. From here we conclude

$$S_{\text{eff,hyp}}^{\text{tail}} = -\frac{GE}{(d-4)_{\text{UV}}}\,\Delta E_{\text{hyp}}(J,\mathcal{E}) + \cdots\,, \tag{4.8}$$

evaluated on hyperbolic orbits. The above expressions connect the total radiated energy to the ultraviolet pole in the effective action due to tail effects. As we shall see, this universal relation can be used to extend the B2B dictionary to the conservative sector, and vice versa.

4.2 Effective to radial action

In order to use the relation in (4.8) we must first connect the value of the effective action to the radial action. This can be achieved by using Hamilton-Jacobi's approach to the motion with the effective action as the generating functional. By choosing the $\theta = \pi/2$ plane, going to the center-of-mass, and isolating conserved quantities, we have

$$S_{\text{eff}} = -E \int dt + J \int d\varphi + 2\pi \mathcal{S}_{r,\text{hyp}}\,, \tag{4.9}$$

where the radial action evaluated on hyperbolic motion is given by

$$\mathcal{S}_{r,\text{hyp}} = \frac{2}{2\pi} \int_{\tilde{r}_-}^{\infty} p_r dr \,, \tag{4.10}$$

and the factor of $1/2\pi$ added for convenience. Hence, at leading order in the tail expansion,

$$\mathcal{S}_{r,\text{hyp}}^{\text{tail}} = \frac{1}{2\pi} S_{\text{eff,hyp}}^{\text{tail}} \,. \tag{4.11}$$

We can also prove the relationship in (4.11) directly from the definition in (4.10). Let us start by separating the potential and tail contributions to the square of the center-of-mass momentum as

$$\boldsymbol{p}^2 = p_\infty^2 + \boldsymbol{p}_{\text{pot}}^2(r, \mathcal{E}) + \boldsymbol{p}_{\text{tail}}^2(r, \mathcal{E}) \,, \tag{4.12}$$

such that, to leading order in the tail expansion,

$$(\delta p_r)_{\text{tail}} = \frac{1}{2} \frac{\boldsymbol{p}_{\text{tail}}^2}{p_r} + \cdots \,. \tag{4.13}$$

We can then compute the correction to the radial action,

$$\mathcal{S}_r^{\text{tail}} = \frac{1}{2\pi} \int_{-\infty}^{+\infty} \dot{r} dt \, (\delta p_r)_{\text{tail}} = \frac{1}{2\pi} \int_{-\infty}^{+\infty} dt \left(\frac{\partial H_{\text{pot}}}{\partial \boldsymbol{p}^2} \right) \boldsymbol{p}_{\text{tail}}^2 + \cdots \,, \tag{4.14}$$

where we used (3.2) and H_{pot} is the Hamiltonian from potential modes. Finally, we must express the momentum in terms of the tail Hamiltonian. Using the relationship [1],

$$\sqrt{\boldsymbol{p}^2 - \boldsymbol{p}_{\text{pot}}^2(r, \mathcal{E}) - \boldsymbol{p}_{\text{tail}}^2(r, \mathcal{E}) + m_1^2} + \sqrt{\boldsymbol{p}^2 - \boldsymbol{p}_{\text{pot}}^2(r, \mathcal{E}) - \boldsymbol{p}_{\text{tail}}^2(r, \mathcal{E}) + m_2^2} = H_{\text{pot}} + H_{\text{tail}} \tag{4.15}$$

we have

$$H_{\text{tail}} = - \left(\frac{\partial H_{\text{pot}}}{\partial \boldsymbol{p}^2} \right) \boldsymbol{p}_{\text{tail}}^2(r, \mathcal{E}) + \cdots \,, \tag{4.16}$$

hence

$$\mathcal{S}_{r,\text{hyp}}^{\text{tail}} = -\frac{1}{2\pi} \int_{-\infty}^{+\infty} H_{\text{tail}} \, dt = \frac{1}{2\pi} S_{\text{eff,hyp}}^{\text{tail}} \,, \tag{4.17}$$

at leading order in the tail expansion, yet to all PN orders, as anticipated.

The case of elliptic-like motion is a tad more subtle. It is straightforward to arrive at the same condition as in (4.7) for the effective action, however, the connection to the radial action is less direct since the latter involves an integral over a period, whereas the effective action is integrated between minus and plus infinity. Nevertheless, we can follow the exact same steps as above using the tail Hamiltonian integrated over only one period of the bound orbit, thus arriving at a similar relationship as in (4.8)

$$\mathcal{S}_{r,\text{ell}}^{\text{tail}} = \frac{2}{2\pi} \int_{r_-}^{r_+} p_r dr = -\frac{GE}{2\pi(d-4)_{\text{UV}}} \Delta E_{\text{ell}}(J, \mathcal{E}) + \cdots \,. \tag{4.18}$$

The reader will now immediately realize that the above imply that the pole in the radial/effective action transforms into a similar pole in the tail Hamiltonian,

$$\frac{H_{\text{tail}}(r, \boldsymbol{p}^2)}{GE} = \frac{\mathcal{F}_E^{\text{src}}(r, \boldsymbol{p}^2)}{(d-4)_{\text{UV}}} + \cdots , \qquad (4.19)$$

from which we can read off the (averaged) flux for generic orbits.

Notice the existence of an isotropic gauge for the local-in-time piece of the tail Hamiltonian implies that the flux may be written solely as a function of r and $\boldsymbol{p}^2$ (for non-spinning bodies). There is, nonetheless, an important difference with the representation in §3.4 regarding the variables used to evaluate the flux. While we use $(r, \mathcal{E})$ in §3.4, the derivation from the tail Hamiltonian involves $(r, \boldsymbol{p}^2)$. This difference simply results in a mismatch for the coefficients of the PM expansion, which can be easily reconstructed from each other.

4.3 Local-in-time

We can now use the B2B map unveiled in (3.9), and following the manipulations in (4.8)-(4.18), we arrive at

$$\mathcal{S}_{r,\text{ell}}^{\text{tail,pole}}(J, \mathcal{E}) = \mathcal{S}_{r,\text{hyp}}^{\text{tail,pole}}(J, \mathcal{E}) - \mathcal{S}_{r,\text{hyp}}^{\text{tail,pole}}(-J, \mathcal{E}) . \qquad (4.20)$$

Since the pole contributes to the local-in-time dynamics, we conclude that the latter respects the original B2B dictionary. Furthermore, by performing a multipole expansion of the tail contribution to the effective action and using the B2B link for the radiated energy at each PN order, it is also straightforward to show the B2B correspondence applies to all local-in-time tail effects. Needless to say, the converse is also manifestly true. Following the steps described in [1, 2] for all local-in-time contributions to the PM expansion of the center-of-mass momentum, we find that the B2B map between angle and periastron advance remains valid, hence the map in (4.20), which in this case would yield (3.9) as a side product.

To complete our discussion of local-in-time effects we must also include conservative memory contributions. However, despite its radiative origin, these can be described by the standard Firsov representation, and therefore naturally obeys the original B2B correspondence. We will add a few comments about isolating the conservative part of the memory in §6.

As a consequence, we find

$$\mathcal{S}_{r,\text{ell}}^{\text{loc}}(J, \mathcal{E}) = \mathcal{S}_{r,\text{hyp}}^{\text{loc}}(J, \mathcal{E}) - \mathcal{S}_{r,\text{hyp}}^{\text{loc}}(-J, \mathcal{E}) . \qquad (4.21)$$

for all local-in-time dynamics, either from potential, tail or memory effects, and generic orbits.

Before moving on, let us stress an important point. At first sight the local-in-time dynamics may appear to include also contributions depending on $\log r$. The latter enters in the computation of the conservative dynamics involving potential-only modes [54, 55]. In principle, one can readily incorporate these effects in the B2B map of (4.21). However,

this $\log r$ is spurious and is only due to the split into regions.[7] There are, nonetheless, crucial logarithmic corrections to the radial action, but involving instead the binding energy (see below). Because of these reasons, it has become customary in the PN literature, e.g. [58, 60], to define the non-local-in-time contribution to the effective action from the (leading) tail as follows

$$S_{\text{eff}}^{\text{nloc}} \equiv -GE \int \frac{dE_{\text{src}}}{d\omega} \log(4r^2\omega^2 e^{\gamma_E})d\omega \,, \tag{4.22}$$

mixing the logarithmic terms from both potential and radiation modes (The factor of e^{γ_E} and $\log 2$ are follow the PN conventions.) In this fashion, all the other pieces are collected as local-in-time contributions which are thus devoid of any logarithmic correction. As we have shown in (4.7), the expression in (4.22) retains its universal character in a PM scheme and therefore it can be generally adopted to describe non-local-in-time effects. We will use this definition in what follows.

4.4 Large-eccentricity limit

At this point the reader may wonder whether the B2B dictionary can remain valid also for the non-local-in-time dynamics induced by (4.22). As we demonstrate in what follows, that is indeed the case. However, there is a major caveat. The B2B map only holds in the limit of large angular momentum. In order to demonstrate this, we start by re-writing the expression in (4.22) in terms of a non-local Hamiltonian,

$$\mathcal{S}_{r,\text{hyp}}^{\text{nloc}}(J,\mathcal{E}) = -\frac{2}{2\pi} \int_{\tilde{r}_-}^{\infty} H_{\text{nloc}}(r,J,\mathcal{E})\frac{dr}{\dot{r}} \,. \tag{4.23}$$

In light of our previous manipulations with the fluxes in §3, and depending on the given J-parity of H_{nloc}, it is clear a B2B-type correspondence must apply. Indeed, we find

$$H_{\text{nloc}}(r,J,\mathcal{E}) = +H_{\text{nloc}}(r,-J,\mathcal{E}) \,, \tag{4.24}$$

in the large J expansion, such that in this particular limit the relation in (4.21) remains the same for non-local-in-time terms, which implies for the full radial action

$$\mathcal{S}_{r,\text{ell}}^{\text{full}}(J,\mathcal{E}) = \mathcal{S}_{r,\text{hyp}}^{\text{full}}(J,\mathcal{E}) - \mathcal{S}_{r,\text{hyp}}^{\text{full}}(-J,\mathcal{E}) \,. \tag{4.25}$$

The proof of (4.24) proceeds as follows. As discussed in e.g. [58, 60, 66], after truncating the derivation of the non-local (conservative) Hamiltonian to a given order in the PN/PM expansion, one can then construct an *effectively local* counter-part describing the evolution of the system to the same PN/PM order. Once the effective Hamiltonian evaluated for unbound motion is known, we can then construct an isotropic gauge in which the latter becomes a function of r and $\boldsymbol{p}^2$ only, which then fulfills the condition in (4.24). (The condition in (4.24) is also satisfied for the gauges in which $(H_{\text{nloc}})_{\text{eff}}$ is given as a function of $r, \boldsymbol{p}^2, p_r^2$.)

---

[7]The spurious nature is also manifest in the lack of factors of $\log J$ (or $\log b$'s) in the total unbound radial action. After noticing that the $\log J$'s are directly linked to the poles arising in the $d \to 4$ limit, their disappearance is ultimately rooted in the same cancelation between infrared/ultraviolet divergences.

4.5 Logarithms

Unlike local effects, non-local tail interactions cause the B2B radial action in the large-eccentricity limit fail to describe generic bound orbits. In particular, non-local terms yield different values for hyperbolic-like and (the more phenomenologically relevant case of) quasi-circular motion. However, somewhat remarkably, the large-eccentricity limit does captures certain non-local contributions for generic orbits, even those with small eccentricities, notably those involving the (leading) logarithms in the binding energy. These terms inherit the universal structure in (4.8) and (4.18), yielding (with $v_\infty \equiv \sqrt{\gamma^2 - 1}$)

$$\frac{\mathcal{S}_{r,\mathrm{hyp/ell}}^{\log}}{GM^2\nu} = -\frac{\Gamma}{\pi\nu}\frac{\Delta E_{\mathrm{hyp/ell}}}{M}\log|v_\infty|, \tag{4.26}$$

which is the left over after the cancelation of logarithms in the angular momentum accompanying the IR/UV poles. They can also be shown to appear directly from the scaling with the velocity of radiation modes, see [26, 27]. Using the map between total radiated energy in (3.9) the B2B relation in (4.21) is thus manifest. As a result, not only all of the local-in-time effects may be readily mapped between unbound and bound motion for generic orbits, also the trademark logarithmic terms. Furthermore, the latter are related by the same B2B formulae derived in [1, 2].

5 Post-Newtonian/Minkowskian

We provide here extensive evidence for the validity of the extended B2B map within the realm of the PN and PM expansions. Let us remind the reader of the definitions

$$\epsilon \equiv -2\mathcal{E} = -2\left(\frac{E-M}{M\nu}\right), \qquad j \equiv \frac{J}{GM^2\nu}, \qquad \ell \equiv \frac{L}{GM^2\nu}, \qquad \tilde{a}_\pm \equiv \frac{1}{GM}(a_1 \pm a_2), \tag{5.1}$$

for the reduced binding energy and total, orbital and spin (canonical) angular momentum, respectively. Finite size effects due to spin are parameterized in terms of the $\kappa_\pm$ parameters introduced in [25]. For the sake of notation, we do not distinguish here between e and $\tilde{e}$ for hyperbolic- and elliptic-like motion. Moreover, for convenience, some of the terms below are written in terms of the *Newtonian* eccentricity $e_N^2 \equiv 1 + 2\mathcal{E}j^2$ [63]. (Since $e = e_N + \cdots$, this is simply a reshuffling of various coefficients in the $1/j$ expansion.) To emphasize the PN orders we will use the following color coding: 0PN, 1PN, 2PN, 3PN, 4PN, 5PN, 6PN.

5.1 Radiated energy

The spin-independent radiated energy due to the source multipole moments (without including tail terms) has been computed to 3PN, both for hyperbolic [63] and elliptic [67]. The results can be written as a function of e_N, j, and $\mathcal{E}$ as follows

$$\Delta E_{\mathrm{hyp}}(j,\mathcal{E}) = \frac{M\nu^2}{15}\left[\frac{850\sqrt{2}\sqrt{\mathcal{E}}}{j^6} + \frac{2692\sqrt{2}\mathcal{E}^{3/2}}{3j^4} + \left(\frac{850}{j^7} + \frac{1464\mathcal{E}}{j^5} + \frac{296\mathcal{E}^2}{j^3}\right)\cos^{-1}\left(-\frac{1}{e_N}\right)\right] \tag{5.2}$$

$$+ \frac{\sqrt{2}\mathcal{E}^{5/2}(2506431 - 3009160\nu)}{105(1 + 2\mathcal{E}j^2)j^4} + \frac{\mathcal{E}^{3/2}(182337 - 140480\nu)}{3\sqrt{2}(1 + 2\mathcal{E}j^2)j^6} - \frac{7\sqrt{\mathcal{E}}(-5763 + 3220\nu)}{2\sqrt{2}(1 + 2\mathcal{E}j^2)j^8}$$

$$- \frac{2\sqrt{2}\mathcal{E}^{7/2}(-89907 + 156380\nu)}{35(1 + 2\mathcal{E}j^2)j^2} + \left(\frac{\mathcal{E}\left(\frac{33885}{2} - 15900\nu\right)}{j^7} + \frac{\mathcal{E}^2\left(\frac{46617}{7} - 10464\nu\right)}{j^5} \right.$$

$$+ \frac{\frac{40341}{4} - 5635\nu}{j^9} + \left. \frac{\mathcal{E}^3\left(\frac{4786}{7} - 888\nu\right)}{j^3} \right) \cos^{-1}\left(-\frac{1}{e_N}\right)$$

$$+ \frac{2\sqrt{2}\mathcal{E}^{11/2}\left(2039036 - 4763297\nu + 6219570\nu^2\right)}{245(1 + 2\mathcal{E}j^2)^2} + \frac{\sqrt{\mathcal{E}}\left(29198255 - 32514426\nu + 6906060\nu^2\right)}{168\sqrt{2}(1 + 2\mathcal{E}j^2)^2 j^{10}}$$

$$+ \frac{\mathcal{E}^{3/2}\left(605244551 - 845377092\nu + 233615340\nu^2\right)}{756\sqrt{2}(1 + 2\mathcal{E}j^2)^2 j^8} + \frac{\mathcal{E}^{5/2}\left(6449654885 - 13029505497\nu + 4951304820\nu^2\right)}{5670\sqrt{2}(1 + 2\mathcal{E}j^2)^2 j^6}$$

$$+ \frac{\sqrt{2}\mathcal{E}^{9/2}\left(208988912 - 6547442643\nu + 6196124970\nu^2\right)}{19845(1 + 2\mathcal{E}j^2)^2 j^2} + \frac{\mathcal{E}^{7/2}\left(9310241671 - 39312545895\nu + 22349042100\nu^2\right)}{19845\sqrt{2}(1 + 2\mathcal{E}j^2)^2 j^4}$$

$$+ \left(\frac{5\mathcal{E}^4}{21j^3}\left(8344 - 7179\nu + 7770\nu^2\right) + \frac{1}{j^{11}}\left(\frac{29198255}{336} - \frac{774153\nu}{8} + \frac{82215\nu^2}{4}\right) \right.$$

$$+ \frac{\mathcal{E}^3}{j^5}\left(\frac{59900}{21} - \frac{219314\nu}{7} + 38412\nu^2\right) + \frac{\mathcal{E}}{j^9}\left(\frac{11947909}{108} - \frac{2838577\nu}{12} + 85995\nu^2\right)$$

$$+ \left. \frac{5\mathcal{E}^2}{252j^7}\left(736055 - 7764219\nu + 5348700\nu^2\right) \right) \cos^{-1}\left(-\frac{1}{e_N}\right)$$

$$+ \frac{\mathcal{E}^{9/2}}{2910600\sqrt{2}(1 + 2\mathcal{E}j^2)^3 j^4}\left(388429282846397 - 2640\left(58245623491 + 813280797\pi^2\right)\nu \right.$$

$$+ 161210743695540\nu^2 - \left. 51997288820400\nu^3 \right) + \frac{\mathcal{E}^{11/2}}{1455300\sqrt{2}(1 + 2\mathcal{E}j^2)^3 j^2}\left(84259836657351 \right.$$

$$- 220\left(7446870460 + 5591391687\pi^2\right)\nu + 36932569900380\nu^2 - \left. 18771891415200\nu^3\right)$$

$$+ \frac{\mathcal{E}^{13/2}}{2182950\sqrt{2}(1 + 2\mathcal{E}j^2)^3}\left(20497310013607 - 220\left(-32611235596 + 2325312171\pi^2\right)\nu \right.$$

$$+ 10835961651900\nu^2 - \left. 9517996719000\nu^3\right) + \frac{\mathcal{E}^{7/2}}{317520\sqrt{2}(1 + 2\mathcal{E}j^2)^3 j^6}\left(49134463233397 \right.$$

$$+ 8\left(-4148934390079 + 7132373325\pi^2\right)\nu + 18910687025664\nu^2 - \left. 4244390811360\nu^3\right)$$

$$+ \frac{\mathcal{E}^{5/2}}{151200\sqrt{2}(1 + 2\mathcal{E}j^2)^3 j^8}\left(14498840196199 + 20\left(-622188698008 + 4083668757\pi^2\right)\nu \right.$$

$$+ 5075295687000\nu^2 - \left. 844365060000\nu^3\right) + \frac{\mathcal{E}^{3/2}}{302400\sqrt{2}(1 + 2\mathcal{E}j^2)^3 j^{10}}\left(9133770967709 \right.$$

$$+ 1100\left(-8061884522 + 70585641\pi^2\right)\nu + 2888074488600\nu^2 - \left. 371614824000\nu^3\right)$$

$$+ \frac{\mathcal{E}^{15/2}j^2}{24255\sqrt{2}(1 + 2\mathcal{E}j^2)^3}\left(744936393 - 5027892760\nu + 9355109148\nu^2 - 10875359880\nu^3\right)$$

$$+ \frac{\sqrt{\mathcal{E}}\left(153014201249 + 440\left(-361091813 + 3587787\pi^2\right)\nu + 43750060200\nu^2 - 4482324000\nu^3\right)}{40320\sqrt{2}(1 + 2\mathcal{E}j^2)^3 j^{12}}$$

$$+ \left(\frac{\mathcal{E}^2}{j^9}\left(\frac{178442872459}{30240} - \frac{5}{432}\left(142791046 + 2595915\pi^2\right)\nu + \frac{23677969\nu^2}{12} - 607110\nu^3\right) \right.$$

$$+\frac{\mathcal{E}^3}{j^7}\left(\frac{10364987867}{5040}+\left(\frac{119338465}{378}-\frac{259735\pi^2}{8}\right)\nu+\frac{19930745\nu^2}{28}-444125\nu^3\right)$$

$$+\frac{\mathcal{E}}{j^{11}}\left(\frac{137076707247}{22400}+\frac{11}{224}\left(-84607982+488187\pi^2\right)\nu+\frac{30107727\nu^2}{16}-\frac{635985\nu^3}{2}\right)$$

$$+\frac{\mathcal{E}^4}{j^5}\left(\frac{11296885277}{92400}+\left(\frac{534595}{14}-\frac{12177\pi^2}{4}\right)\nu+\frac{2595759\nu^2}{28}-103395\nu^3\right)$$

$$+\frac{1}{j^{13}}\left(\frac{25574348567}{11520}+\frac{11\left(-361091813+3587787\pi^2\right)\nu}{2016}+\frac{17361135\nu^2}{32}-\frac{444675\nu^3}{8}\right)$$

$$+\frac{\mathcal{E}^5}{j^3}\left(\frac{2075735}{1848}-\frac{11920\nu}{3}+\frac{45467\nu^2}{14}-3256\nu^3\right)\Bigg)\cos^{-1}\left(-\frac{1}{e_N}\right)$$

$$+\left(\frac{161249\sqrt{2}\sqrt{\mathcal{E}}}{j^{12}}+\frac{7455118\sqrt{2}\mathcal{E}^{3/2}}{15j^{10}}+\frac{6414436\sqrt{2}\mathcal{E}^{5/2}}{15j^8}+\frac{140201672\sqrt{2}\mathcal{E}^{7/2}}{1575j^6}\right)\log\left(\frac{2\mathcal{E}}{e_N}\right)$$

$$+\left(-\frac{161249}{j^{13}}-\frac{3022536\mathcal{E}}{5j^{11}}-\frac{2104904\mathcal{E}^2}{3j^9}-\frac{5406496\mathcal{E}^3}{21j^7}-\frac{508464\mathcal{E}^4}{35j^5}\right)$$

$$\times\left(\text{Cl}_2\left(2\cos^{-1}\left(-\frac{1}{e_N}\right)\right)+\cos^{-1}\left(-\frac{1}{e_N}\right)\log\left(\frac{2(e_N^2-1)}{e_N\,\mathcal{E}}\right)\right)\Bigg].$$

The Clausen function of order 2 is defined by the integral representation,

$$\text{Cl}_2(z)\equiv-\int_0^z dy\,\log\left|2\sin\frac{y}{2}\right|.\tag{5.3}$$

On the other hand, for a period of an elliptic orbit we have

$$\Delta E_{\text{ell}}(j,\mathcal{E})=\frac{M\,\nu^2}{15}\left[\frac{850\pi}{j^7}+\frac{1464\mathcal{E}\pi}{j^5}+\frac{296\mathcal{E}^2\pi}{j^3}+\frac{\mathcal{E}^2\pi}{j^5}\left(\frac{46617}{7}-10464\nu\right)\right.\tag{5.4}$$

$$+\frac{7\pi(5763-3220\nu)}{4j^9}+\frac{15\mathcal{E}\pi(2259-2120\nu)}{2j^7}+\frac{\mathcal{E}^3\pi}{j^3}\left(\frac{4786}{7}-888\nu\right)$$

$$+\frac{5\mathcal{E}^4\pi\left(8344-7179\nu+7770\nu^2\right)}{21j^3}+\frac{2\mathcal{E}^3\pi\left(29950-328971\nu+403326\nu^2\right)}{21j^5}$$

$$+\frac{5\mathcal{E}^2\pi\left(736055-7764219\nu+5348700\nu^2\right)}{252j^7}+\frac{\pi\left(29198255-32514426\nu+6906060\nu^2\right)}{336j^{11}}$$

$$+\frac{\mathcal{E}\pi\left(11947909-25547193\nu+9287460\nu^2\right)}{108j^9}$$

$$-\frac{161249\sqrt{2}\sqrt{-\mathcal{E}}\pi}{j^{12}}-\frac{7455118\sqrt{2}\sqrt{-\mathcal{E}}\mathcal{E}\pi}{15j^{10}}-\frac{6414436\sqrt{2}\sqrt{-\mathcal{E}}\mathcal{E}^2\pi}{15j^8}$$

$$-\frac{140201672\sqrt{2}\sqrt{-\mathcal{E}}\mathcal{E}^3\pi}{1575j^6}+\frac{\mathcal{E}\pi}{22400j^{11}}\left(137076707247+1100\left(-84607982+488187\pi^2\right)\nu\right.$$

$$+42150817800\nu^2-7123032000\nu^3\Big)+\frac{\pi}{80640j^{13}}\left(179020439969\right.$$

$$+440\left(-361091813+3587787\pi^2\right)\nu+43750060200\nu^2-4482324000\nu^3\Big)$$

$$+\frac{\mathcal{E}^5\pi}{j^3}\left(\frac{2075735}{1848}-\frac{11920\nu}{3}+\frac{45467\nu^2}{14}-3256\nu^3\right)$$

$$+\frac{\mathcal{E}^2}{j^9}\left(-\frac{1}{16}\left(480725\pi^3\nu\right)+\pi\left(\frac{178442872459}{30240}-\frac{356977615\nu}{216}+\frac{23677969\nu^2}{12}-607110\nu^3\right)\right)$$

$$+\frac{\mathcal{E}^3}{j^7}\left(-\frac{1}{8}\left(259735\pi^3\nu\right)+\pi\left(\frac{10364987867}{5040}+\frac{119338465\nu}{378}+\frac{19930745\nu^2}{28}-444125\nu^3\right)\right)$$

$$+\frac{\mathcal{E}^4}{j^5}\left(-\frac{1}{4}\left(12177\pi^3\nu\right)+\pi\left(\frac{11296885277}{92400}+\frac{534595\nu}{14}+\frac{2595759\nu^2}{28}-103395\nu^3\right)\right)$$

$$+\left(\frac{161249\pi}{j^{13}}+\frac{3022536\mathcal{E}\pi}{5j^{11}}+\frac{2104904\mathcal{E}^2\pi}{3j^9}+\frac{5406496\mathcal{E}^3\pi}{21j^7}+\frac{508464\mathcal{E}^4\pi}{35j^5}\right)\times\log\left(\frac{(1+\sqrt{1-e_N^2})\mathcal{E}}{2(e_N^2-1)}\right)\Bigg].$$

In order to apply the B2B correspondence in (3.9) we must exercise some care with the analytic continuation in the angular momentum and binding energy. In particular, notice that we have expanded the polynomial factors in $1/j$ explicitly, while keeping the special functions in terms of the eccentricity. For the latter we apply the analytic continuation according to the B2B dictionary using the definition of the principal values, e.g.

$$\cos^{-1}(z)=-i\,\log\left(z+i\sqrt{1-z^2}\right),\tag{5.5}$$

such that

$$\cos^{-1}\left(\frac{1}{e}\right)+\cos^{-1}\left(-\frac{1}{e}\right)=\pi,\quad\log\left(\frac{1}{e}\right)-\log\left(-\frac{1}{e}\right)=i\,\pi,\tag{5.6}$$

gives the relation

$$\cos^{-1}\left(-\frac{1}{e}\right)\log\left(\frac{2(e^2-1)}{e\,\mathcal{E}}\right)+\cos^{-1}\left(\frac{1}{e}\right)\log\left(-\frac{2(e^2-1)}{e\,\mathcal{E}}\right)$$

$$=\cos^{-1}\left(-\frac{1}{e}\right)\left(\log\left(\frac{2(e^2-1)}{e\,\mathcal{E}}\right)-\log\left(-\frac{2(e^2-1)}{e\,\mathcal{E}}\right)\right)+\pi\,\log\left(-\frac{2(e^2-1)}{e\,\mathcal{E}}\right)$$

$$=\cos^{-1}\left(-\frac{1}{e}\right)i\,\pi+\pi\,\log\left(-\frac{2(e^2-1)}{e\,\mathcal{E}}\right)=\pi\log\left(-\frac{1}{e}+i\sqrt{1-\frac{1}{e^2}}\right)+\pi\,\log\left(-\frac{2(e^2-1)}{e\,\mathcal{E}}\right)$$

$$=\pi\,\log\left(-2\frac{(1-\sqrt{1-e^2})(1-e^2)}{e^2\mathcal{E}}\right)=-\pi\,\log\left(\frac{(1+\sqrt{1-e^2})\mathcal{E}}{2(e^2-1)}\right),\tag{5.7}$$

which links hyperbolic and elliptic orbits. Another important relation is given by

$$\text{Cl}_2\left(2\,\cos^{-1}\left(\frac{-1}{e}\right)\right)+\text{Cl}_2\left(2\,\cos^{-1}\left(\frac{1}{e}\right)\right)=0\,,\tag{5.8}$$

which altogether disappears from the elliptic case. This is proved by noticing

$$\text{Cl}_2\left(2\,\cos^{-1}\left(\frac{-1}{e}\right)\right)=\text{Cl}_2\left(2\,\pi-2\,\cos^{-1}\left(\frac{1}{e}\right)\right)$$

$$=-\int_0^{2\,\pi-2\,\cos^{-1}\left(\frac{1}{e}\right)}dz\,\log\left|2\sin\frac{z}{2}\right|=-\int_{-2\pi}^{-2\,\cos^{-1}\left(\frac{1}{e}\right)}dz\,\log\left|2\sin\frac{z+2\pi}{2}\right|$$

$$=-\int_0^{2\,\pi}dz\,\log\left|2\sin\frac{z}{2}\right|-\int_0^{-2\,\cos^{-1}\left(\frac{1}{e}\right)}dz\,\log\left|2\sin\frac{2\pi+z}{2}\right|$$

$$=-\int_0^{-2\,\cos^{-1}\left(\frac{1}{e}\right)}dz\,\log\left|2\sin\frac{z}{2}\right|=\int_0^{2\,\cos^{-1}\left(\frac{1}{e}\right)}dz\,\log\left|2\sin\frac{z}{2}\right|$$

$$= -\mathrm{Cl}_2\left(2\cos^{-1}\left(\frac{1}{e}\right)\right) \tag{5.9}$$

where we used the identity $\int_0^{2\pi} dz\,\log|2\sin\frac{z}{2}| = 0$.

Other terms, such as those involving $\sqrt{\mathcal{E}}$, produce imaginary pieces for bound orbits which are either canceled against similar complex terms or by the B2B relations. After all of these manipulations, we find that the B2B correspondence in (3.9) is neatly fulfilled to 3PN order. A similar check was discussed in [17] in the context of the PM expansion. We confirm the results in [17] are consistent with the PN values presented here.

5.2 Radiated angular momentum

The same logic applies to the angular momentum. For non-spinning bodies we find

$$
\begin{aligned}
\Delta J_{\mathrm{hyp}}(j,\mathcal{E}) = \frac{8\,G\,M^2\,\nu^2}{5}&\left[\frac{15\sqrt{2}\sqrt{\mathcal{E}}}{j^3} + \frac{4\sqrt{2}\mathcal{E}^{3/2}}{j} + \left(\frac{15}{j^4} + \frac{14\mathcal{E}}{j^2}\right)\cos^{-1}\left(-\frac{1}{e_N}\right)\right. \\
&+\frac{\mathcal{E}^{3/2}\left(5541\sqrt{2} - 8620\sqrt{2}\nu\right)}{72j^3} + \frac{\sqrt{\mathcal{E}}\left(4953\sqrt{2} - 4748\sqrt{2}\nu\right)}{48j^5} + \frac{\mathcal{E}^{5/2}\left(109\sqrt{2} - 35\sqrt{2}\nu\right)}{7j} \\
&+\frac{\sqrt{\mathcal{E}}\left(9\sqrt{2} + \sqrt{2}\nu\right)}{(1 + 2\mathcal{E}j^2)j^5} + \left(\frac{\mathcal{E}^2(4283 - 3976\nu)}{84j^2} + \frac{\mathcal{E}(535 - 748\nu)}{4j^4} - \frac{5(-1077 + 940\nu)}{48j^6}\right)\cos^{-1}\left(-\frac{1}{e_N}\right) \\
&+\frac{\sqrt{\mathcal{E}}\left(123507\sqrt{2} - 23678\sqrt{2}\nu - 2289\sqrt{2}\nu^2\right)}{1344(1 + 2\mathcal{E}j^2)j^7} + \frac{\sqrt{\mathcal{E}}\left(-81\sqrt{2} - 18\sqrt{2}\nu - \sqrt{2}\nu^2\right)}{8(1 + 2\mathcal{E}j^2)^2 j^7} \\
&+\frac{\mathcal{E}^{7/2}\left(3245\sqrt{2} - 5886\sqrt{2}\nu + 3213\sqrt{2}\nu^2\right)}{504j} + \frac{\mathcal{E}^{5/2}\left(-439377\sqrt{2} - 1828552\sqrt{2}\nu + 2246335\sqrt{2}\nu^2\right)}{5040j^3} \\
&+\frac{\sqrt{\mathcal{E}}\left(15340289\sqrt{2} - 38231694\sqrt{2}\nu + 14143059\sqrt{2}\nu^2\right)}{36288j^7} \\
&+\frac{\mathcal{E}^{3/2}\left(-12397361\sqrt{2} - 59811138\sqrt{2}\nu + 53024895\sqrt{2}\nu^2\right)}{54432j^5} \\
&+\left(\frac{\mathcal{E}^3\left(5308 - 32877\nu + 28308\nu^2\right)}{252j^2} + \frac{5\mathcal{E}\left(-2999 - 152946\nu + 106848\nu^2\right)}{432j^6}\right. \\
&\left.+\frac{1307683 - 2782332\nu + 1005480\nu^2}{2592j^8} + \frac{\mathcal{E}^2\left(-404980 - 1181889\nu + 1438668\nu^2\right)}{1512j^4}\right)\cos^{-1}\left(-\frac{1}{e_N}\right) \\
&+\left(\frac{3531\sqrt{\mathcal{E}}}{\sqrt{2}j^9} + \frac{10700\sqrt{2}\mathcal{E}^{3/2}}{3j^7} + \frac{421366\sqrt{2}\mathcal{E}^{5/2}}{315j^5}\right)\log\left(\frac{2\,\mathcal{E}}{e_N}\right) \\
&-\left(\frac{3531}{2j^{10}} + \frac{14231\mathcal{E}}{3j^8} + \frac{21614\mathcal{E}^2}{7j^6} + \frac{9844\mathcal{E}^3}{35j^4}\right)\left(\log\left(\frac{2(e_N^2 - 1)}{e_N\,\mathcal{E}}\right)\cos^{-1}\left(-\frac{1}{e_N}\right) + \mathrm{Cl}_2\left(2\cos^{-1}\left(-\frac{1}{e_N}\right)\right)\right) \\
&+\frac{\mathcal{E}^{5/2}}{2177280j^5}\left(10005567679\sqrt{2} + (6156118418\sqrt{2} - 202155912\sqrt{2}\pi^2)\nu + 12209691726\sqrt{2}\nu^2\right. \\
&\left.-10620524250\sqrt{2}\nu^3\right) + \frac{\mathcal{E}^{3/2}}{1451520j^7}\left(24486609623\sqrt{2} + (-18545026170\sqrt{2} + 252462420\sqrt{2}\pi^2)\nu\right. \\
&\left.+18259461090\sqrt{2}\nu^2 - 6662875590\sqrt{2}\nu^3\right) + \frac{\sqrt{\mathcal{E}}}{2903040j^9}\left(37783086543\sqrt{2}\right. \\
&\left.+(-52725330410\sqrt{2} + 834567300\sqrt{2}\pi^2)\nu + 19852063650\sqrt{2}\nu^2 - 3342659670\sqrt{2}\nu^3\right)
\end{aligned} \tag{5.10}
$$

$$+\frac{\mathcal{E}^{7/2}}{282240 j^3}\left(-106774701\sqrt{2}+33275322\sqrt{2}\nu+305926390\sqrt{2}\nu^2-341077730\sqrt{2}\nu^3\right)$$

$$+\frac{\mathcal{E}^{9/2}\left(-6973\sqrt{2}-35695\sqrt{2}\nu+334521\sqrt{2}\nu^2-172557\sqrt{2}\nu^3\right)}{22176 j}$$

$$+\frac{\sqrt{\mathcal{E}}\left(244427427\sqrt{2}-165077725\sqrt{2}\nu+1487808\sqrt{2}\pi^2\nu-6469083\sqrt{2}\nu^2-134379\sqrt{2}\nu^3\right)}{290304(1+2\mathcal{E}j^2)j^9}$$

$$+\frac{\sqrt{\mathcal{E}}\left(729\sqrt{2}+243\sqrt{2}\nu+27\sqrt{2}\nu^2+\sqrt{2}\nu^3\right)}{48(1+2\mathcal{E}j^2)^3 j^9}$$

$$+\frac{\sqrt{\mathcal{E}}\left(-772659\sqrt{2}+48105\sqrt{2}\nu+22507\sqrt{2}\nu^2+847\sqrt{2}\nu^3\right)}{5376(1+2\mathcal{E}j^2)^2 j^9}$$

$$+\left(\frac{\mathcal{E}^2\left(2082786797-44373700\nu-8136450\pi^2\nu+1398279600\nu^2-910576800\nu^3\right)}{120960 j^6}\right.$$

$$+\frac{\mathcal{E}^3\left(90979951+255064600\nu-5811750\pi^2\nu+433045800\nu^2-492912000\nu^3\right)}{151200 j^4}$$

$$+\frac{5567205457-6037270480\nu+94382820\pi^2\nu+2200128840\nu^2-371498400\nu^3}{322560 j^{10}}$$

$$+\frac{\mathcal{E}\left(1737906083-1253646560\nu+18597600\pi^2\nu+889119000\nu^2-277754400\nu^3\right)}{51840 j^8}$$

$$\left.+\frac{\mathcal{E}^4\left(-227005-5072672\nu+11771892\nu^2-9953328\nu^3\right)}{44352 j^2}\right)\cos^{-1}\left(-\frac{1}{e_N}\right)\Bigg],$$

whereas for one period of elliptic motion we have

$$\Delta J_{\text{ell}}(j,\mathcal{E})=\frac{8\,G\,M^2\,\nu^2}{5}\left[\frac{15\pi}{j^4}+\frac{14\mathcal{E}\pi}{j^2}+\left(\frac{\mathcal{E}^2\pi(4283-3976\nu)}{84 j^2}+\frac{\mathcal{E}\pi\left(\frac{535}{4}-187\nu\right)}{j^4}-\frac{5\pi(-1077+940\nu)}{48 j^6}\right)\right.$$

$$+\frac{\mathcal{E}^3\pi\left(5308-32877\nu+28308\nu^2\right)}{252 j^2}+\frac{5\mathcal{E}\pi\left(-2999-152946\nu+106848\nu^2\right)}{432 j^6} \tag{5.11}$$

$$+\frac{\pi\left(1307683-2782332\nu+1005480\nu^2\right)}{2592 j^8}+\frac{\mathcal{E}^2\pi\left(-404980-1181889\nu+1438668\nu^2\right)}{1512 j^4}$$

$$+-\frac{3531\sqrt{-\mathcal{E}}\pi}{\sqrt{2}j^9}-\frac{10700\sqrt{2}\sqrt{-\mathcal{E}}\mathcal{E}\pi}{3 j^7}-\frac{421366\sqrt{2}\sqrt{-\mathcal{E}}\mathcal{E}^2\pi}{315 j^5}$$

$$+\frac{\pi\left(5567205457+20\left(-301863524+4719141\pi^2\right)\nu+2200128840\nu^2-371498400\nu^3\right)}{322560 j^{10}}$$

$$+\frac{\mathcal{E}\pi}{51840 j^8}\left(1737906083+160\left(-7835291+116235\pi^2\right)\nu+889119000\nu^2-277754400\nu^3\right)$$

$$-\frac{\mathcal{E}^4\pi\left(227005+5072672\nu-11771892\nu^2+9953328\nu^3\right)}{44352 j^2}$$

$$-\frac{\mathcal{E}^2\pi\left(-2082786797+350\left(126782+23247\pi^2\right)\nu-1398279600\nu^2+910576800\nu^3\right)}{120960 j^6}$$

$$+\frac{\mathcal{E}^3}{j^4}\left(-\frac{1}{16}\left(615\pi^3\nu\right)+\pi\left(\frac{90979951}{151200}+\frac{182189\nu}{108}+\frac{240581\nu^2}{84}-3260\nu^3\right)\right)$$

$$\left.+\left(\frac{3531\pi}{2 j^{10}}+\frac{14231\mathcal{E}\pi}{3 j^8}+\frac{21614\mathcal{E}^2\pi}{7 j^6}+\frac{9844\mathcal{E}^3\pi}{35 j^4}\right)\log\left(\frac{(1+\sqrt{1-e_N^2})\mathcal{E}}{2\left(e_N^2-1\right)}\right)\right].$$

The reader will notice the odd vs even factors of $1/j$ in the expansions of the energy and angular momentum. As a result, both entail the same type of analytic continuation, such that we find the latter is as well nicely connected by (3.11) to 3PN order.

5.3 Fluxes

The above values for the total radiated energy and angular momentum were computed from the knowledge of the known PN fluxes in the multipole expansion. However, it is also possible to reverse engineer from the total values, in particular for those obtained from the (on-shell) scattering process. As an example of this inverse problem, let us consider the 3PM total radiated energy recently computed through various methodologies in [14, 17, 26, 27, 29, 30, 32, 68],

$$\frac{\Delta E_{\text{hyp}}^{(0)}}{M} = -\frac{2\pi\nu^2}{3}\frac{(\gamma^2 - 1)^2}{\Gamma^4}\chi_{2\epsilon}(\gamma)\,,\tag{5.12}$$

where the expression for $\chi_{2\epsilon}$ can be found in [26, 27]. Following the steps outlined in §3.4, using

$$\int_{J/p_\infty}^{\infty} \frac{J^3}{r^4\sqrt{p_\infty^2 - J^2/r^2}}dr = \frac{\pi}{4}p_\infty^2\,,\tag{5.13}$$

and

$$\frac{\partial H(r, \boldsymbol{p}^2)}{\partial \boldsymbol{p}^2} = \frac{\partial}{\partial \boldsymbol{p}^2}\left(\sqrt{\boldsymbol{p}^2 + m_1^2} + \sqrt{\boldsymbol{p}^2 + m_2^2} + \cdots\right) = \frac{1}{2\xi E} + \mathcal{O}(G)\,,\tag{5.14}$$

we find

$$\mathcal{F}_E^{(0)}(\mathcal{E}) = \frac{2}{\pi}\frac{\nu\Gamma}{\xi(\gamma^2 - 1)}\frac{\Delta E_{\text{hyp}}^{(0)}(\mathcal{E})}{M}\,,\tag{5.15}$$

for the leading coefficient of the PM expansion of the energy flux, see (3.15).

As we discussed earlier, the energy flux can also be obtained through the pole in the tail Hamiltonian, see (4.19). The computation has been carried over in [26, 27] at 4PM order. As we mentioned, there is a caveat regarding the flux as a function of $(r, \boldsymbol{p}^2)$ as in the tail Hamiltonian, and $(r, \mathcal{E})$ as in the representation in §3.4. Yet, the mismatch in the PM coefficients of the G/r expansion only matters at higher orders. Hence, we find

$$\mathcal{F}_E^{(0)}(\mathcal{E}) = -\frac{4}{3}\frac{(\gamma^2 - 1)\nu^3}{\Gamma^3\xi}\chi_{2\epsilon}(\gamma)\,,\tag{5.16}$$

for the 3PM flux, which is equivalent to the result in (5.15). Unfortunately, the 3PM value is not sufficient to recover even the leading PN result from the quadrupole formula. However, it is straightforward to compute the required term in the isotropic gauge, yielding[8]

$$\mathcal{F}_E^{(1)}(\mathcal{E}) = \frac{34\nu^2}{3} + \mathcal{O}(\mathcal{E})\,.\tag{5.17}$$

---

[8]Notice this turns into a factor of $22\nu^2/15$ when the flux is evaluated as a function of the momentum [26].

5.4 Aligned-spin configurations

Using the results for the spin-dependent dynamical effects to next-to-leading order [65, 69–73], recently combined in [57] to compute the associated fluxes (see also [74]), we derived the radiated energy and angular momentum for aligned-spin configurations. To the extent of our knowledge, the following results are reported here for the first time.

For one period of elliptic-like motion we find to next-to-leading PN order and quadratic order in the spins,

$$\frac{\Delta E_{\text{ell}}(\ell, \tilde{a}_\pm, \mathcal{E})}{M\pi\nu^2} = \tag{5.18}$$

$$\frac{1}{\ell^4}\left\{-\frac{4}{5}\mathcal{E}^3[33\tilde{a}_-\Delta + 97\tilde{a}_+] + \frac{1}{70}\mathcal{E}^4[\nu(7504\tilde{a}_-\Delta + 20048\tilde{a}_+) - 4869\tilde{a}_-\Delta - 15806\tilde{a}_+]\right\}$$

$$+ \frac{1}{\ell^5}\left\{\frac{2}{5}\mathcal{E}^3\left[\tilde{a}_-^2(59\kappa_+ - 109) + 118\tilde{a}_-\tilde{a}_+\kappa_- + 59\tilde{a}_+^2(\kappa_+ + 2)\right]\right.$$

$$+ \frac{1}{280}\mathcal{E}^4\left[\nu\left(-56\tilde{a}_-^2(531\kappa_+ - 517) - 59472\tilde{a}_-\tilde{a}_+\kappa_- - 29736\tilde{a}_+^2(\kappa_+ + 2)\right)\right.$$

$$+ \tilde{a}_-^2(609\Delta\kappa_- + 26643\kappa_+ - 38138) + 6\tilde{a}_-\tilde{a}_+(203\Delta\kappa_+ + 6104\Delta + 8881\kappa_-)$$

$$\left.\left. + \tilde{a}_+^2(609\Delta\kappa_- + 26643\kappa_+ + 49478)\right]\right\}$$

$$+ \frac{1}{\ell^6}\left\{-12\mathcal{E}^2[34\tilde{a}_-\Delta + 145\tilde{a}_+] + \frac{1}{42}\mathcal{E}^3[\nu(127456\tilde{a}_-\Delta + 509152\tilde{a}_+) - 114753\tilde{a}_-\Delta - 372729\tilde{a}_+]\right\}$$

$$+ \frac{1}{\ell^7}\left\{\mathcal{E}^2\left[334\tilde{a}_-^2\kappa_+ - 635\tilde{a}_-^2 + 668\tilde{a}_-\tilde{a}_+\kappa_- + 334\tilde{a}_+^2\kappa_+ + 668\tilde{a}_+^2\right]\right.$$

$$+ \frac{1}{84}\mathcal{E}^3\left[\nu\left(-112\tilde{a}_-^2(2037\kappa_+ - 1214) - 456288\tilde{a}_-\tilde{a}_+\kappa_- - 228144\tilde{a}_+^2(\kappa_+ + 2)\right)\right.$$

$$+ \tilde{a}_-^2(22827\Delta\kappa_- + 215028\kappa_+ - 328472) + 6\tilde{a}_-\tilde{a}_+(7609\Delta\kappa_+ + 93156\Delta + 71676\kappa_-)$$

$$\left.\left. + \tilde{a}_+^2(22827\Delta\kappa_- + 215028\kappa_+ + 1010300)\right]\right\}$$

$$+ \frac{1}{\ell^8}\left\{-833\mathcal{E}[\tilde{a}_-\Delta + 5\tilde{a}_+] + \frac{1}{12}\mathcal{E}^2[\nu(136500\tilde{a}_-\Delta + 665364\tilde{a}_+) - 187318\tilde{a}_-\Delta - 651175\tilde{a}_+]\right\}$$

$$+ \frac{1}{\ell^9}\left\{\frac{7}{6}\mathcal{E}\left[\tilde{a}_-^2(539\kappa_+ - 1039) + 1078\tilde{a}_-\tilde{a}_+\kappa_- + 539\tilde{a}_+^2(\kappa_+ + 2)\right]\right.$$

$$+ \frac{7}{48}\mathcal{E}^2\left[\nu\left(-4\tilde{a}_-^2(16099\kappa_+ - 1099) - 128792\tilde{a}_-\tilde{a}_+\kappa_- - 64396\tilde{a}_+^2(\kappa_+ + 2)\right)\right.$$

$$+ \tilde{a}_-^2(9693\Delta\kappa_- + 83685\kappa_+ - 134138) + 2\tilde{a}_-\tilde{a}_+(9693\Delta\kappa_+ + 130688\Delta + 83685\kappa_-)$$

$$\left.\left. + 3\tilde{a}_+^2(3231\Delta\kappa_- + 27895\kappa_+ + 201638)\right]\right\}$$

$$+ \frac{1}{\ell^{10}}\left\{-\frac{21}{5}[93\tilde{a}_-\Delta + 506\tilde{a}_+] + \frac{3}{40}\mathcal{E}[\nu(162988\tilde{a}_-\Delta + 895188\tilde{a}_+) - 328441\tilde{a}_-\Delta - 1285277\tilde{a}_+]\right\}$$

$$
+ \frac{1}{\ell^{11}} \Bigg\{ \frac{63}{20} \left[\tilde{a}_-^2 (88\kappa_+ - 171) + 176\tilde{a}_-\tilde{a}_+\kappa_- + 88\tilde{a}_+^2 (\kappa_+ + 2) \right]
$$
$$
+ \frac{3}{80} \mathcal{E} \left[\nu \left(-196\tilde{a}_-^2 (1296\kappa_+ + 761) - 508032\tilde{a}_-\tilde{a}_+\kappa_- - 254016\tilde{a}_+^2 (\kappa_+ + 2) \right) \right.
$$
$$
+ \tilde{a}_-^2 (48321\Delta\kappa_- + 470006\kappa_+ - 775904) + 2\tilde{a}_-\tilde{a}_+ (48321\Delta\kappa_+ + 770532\Delta + 470006\kappa_-)
$$
$$
\left. + \tilde{a}_+^2 (48321\Delta\kappa_- + 470006\kappa_+ + 4121960) \right] \Bigg\}
$$
$$
+ \frac{1}{\ell^{12}} \left\{ \frac{11 (\nu (387296\tilde{a}_-\Delta + 2308880\tilde{a}_+) - 1097925\tilde{a}_-\Delta - 4756668\tilde{a}_+)}{1120} \right\}
$$
$$
+ \frac{1}{\ell^{13}} \Bigg\{ \frac{11}{4480} \left[\nu \left(-112\tilde{a}_-^2 (10347\kappa_+ + 14269) - 2317728\tilde{a}_-\tilde{a}_+\kappa_- - 1158864\tilde{a}_+^2 (\kappa_+ + 2) \right) \right.
$$
$$
+ \tilde{a}_-^2 (262227\Delta\kappa_- + 2978061\kappa_+ - 5005550) + 6\tilde{a}_-\tilde{a}_+ (87409\Delta\kappa_+ + 1644440\Delta + 992687\kappa_-)
$$
$$
\left. + \tilde{a}_+^2 (262227\Delta\kappa_- + 2978061\kappa_+ + 28885322) \right] \Bigg\}
$$

The computation for unbound orbits is significantly more involved. However, after some massaging it can be written as follows:

$$
\Delta E_{\text{hyp}}(\ell, \tilde{a}_\pm, \mathcal{E}) = + \frac{\Delta E_{\text{ell}}(\ell, \tilde{a}_\pm, \mathcal{E})}{\pi} \cos^{-1} \left(\frac{-1}{e_N} \right) + \Delta E_{\text{hyp}}^{(\text{even})}(\ell, \tilde{a}_\pm, \mathcal{E}), \tag{5.19}
$$

where $\Delta E_{\text{hyp}}^{(\text{even})}$ is even under $J \to -J$ (and $e \to -e$). Hence, noticing that ΔE_{ell} is odd under J-parity, and using (5.6), the B2B map in (3.9) is obeyed.

The explicit expression for the (lengthier) even term is given by:

$$
\frac{\sqrt{2} e_N^4 \Delta E_{\text{hyp}}^{(\text{even})}(\ell, \tilde{a}_\pm, \mathcal{E})}{M\nu^2} = \tag{5.20}
$$
$$
\frac{1}{\ell} \Bigg\{ -\frac{16}{75} \mathcal{E}^{9/2} [5713\tilde{a}_-\Delta + 21521\tilde{a}_+]
$$
$$
+ \frac{2\mathcal{E}^{11/2} [\nu (38147088\tilde{a}_-\Delta + 131474448\tilde{a}_+) - 28359001\tilde{a}_-\Delta - 93954742\tilde{a}_+]}{11025} \Bigg\}
$$
$$
\frac{1}{\ell^2} \Bigg\{ \frac{8}{225} \mathcal{E}^{9/2} \left[\tilde{a}_-^2 (29281\kappa_+ - 55127) + 58562\tilde{a}_-\tilde{a}_+\kappa_- + 29281\tilde{a}_+^2 (\kappa_+ + 2) \right]
$$
$$
+ \frac{\mathcal{E}^{11/2}}{22050} \left[\nu \left(-56\tilde{a}_-^2 (2554367\kappa_+ - 2034713) - 286089104\tilde{a}_-\tilde{a}_+ + \kappa_- - 143044552\tilde{a}_+^2 (\kappa_+ + 2) \right) \right.
$$
$$
+ \tilde{a}_-^2 (9872037\Delta\kappa_- + 123495327\kappa_+ - 183275618)
$$
$$
+ 2\tilde{a}_-\tilde{a}_+ (9872037\Delta\kappa_+ + 130785704\Delta + 123495327\kappa_-)
$$
$$
\left. + 9\tilde{a}_+^2 (1096893\Delta\kappa_- + 13721703\kappa_+ + 44532590) \right] \Bigg\}
$$
$$
\frac{1}{\ell^3} \Bigg\{ -\frac{8}{75} \mathcal{E}^{7/2} [54851\tilde{a}_-\Delta + 252517\tilde{a}_+]
$$
$$
+ \frac{\mathcal{E}^{9/2} [\nu (630281904\tilde{a}_-\Delta + 2806389936\tilde{a}_+) - 702186917\tilde{a}_-\Delta - 2332888208\tilde{a}_+]}{11025} \Bigg\}
$$

$$\frac{1}{\ell^4}\left\{\frac{4}{225}\mathcal{E}^{7/2}\left[\tilde{a}_-^2(259817\kappa_+ - 497014) + 519634\tilde{a}_-\tilde{a}_+\kappa_- + 259817\tilde{a}_+^2(\kappa_+ + 2)\right]\right.$$
$$+ \frac{\mathcal{E}^{9/2}}{44100}\left[\nu\left(-56\tilde{a}_-^2(38656801\kappa_+ - 13673167) - 4329561712\tilde{a}_-\tilde{a}_+\kappa_- - 2164780856\tilde{a}_+^2(\kappa_+ + 2)\right)\right.$$
$$+ \tilde{a}_-^2(271723095\Delta\kappa_- + 2371844217\kappa_+ - 3718678126)$$
$$+ 2\tilde{a}_-\tilde{a}_+(271723095\Delta\kappa_+ + 3450724648\Delta + 2371844217\kappa_-)$$
$$\left.\left.+ 3\tilde{a}_+^2(90574365\Delta\kappa_- + 790614739\kappa_+ + 4794170902)\right]\right\}$$

$$\frac{1}{\ell^5}\left\{-\frac{4}{75}\mathcal{E}^{5/2}[150673\tilde{a}_-\Delta + 755891\tilde{a}_+]\right.$$
$$\left.+ \frac{\mathcal{E}^{7/2}[\nu(1426875492\tilde{a}_-\Delta + 7196110404\tilde{a}_+) - 2221381823\tilde{a}_-\Delta - 8090706680\tilde{a}_+]}{11025}\right\}$$

$$\frac{1}{\ell^6}\left\{\frac{2}{225}\mathcal{E}^{5/2}\left[\tilde{a}_-^2(679831\kappa_+ - 1310552) + 1359662\tilde{a}_-\tilde{a}_+\kappa_- + 679831\tilde{a}_+^2(\kappa_+ + 2)\right]\right.$$
$$+ \frac{\mathcal{E}^{7/2}}{44100}\left[\nu\left(-28\tilde{a}_-^2(165710591\kappa_+ + 18223105) - 9279793096\tilde{a}_-\tilde{a}_+\kappa_- - 4639896548\tilde{a}_+^2(\kappa_+ + 2)\right)\right.$$
$$+ \tilde{a}_-^2(745894737\Delta\kappa_- + 6737032059\kappa_+ - 10910108374)$$
$$+ 2\tilde{a}_-\tilde{a}_+(745894737\Delta\kappa_+ + 10682364952\Delta + 6737032059\kappa_-)$$
$$\left.\left.+ 3\tilde{a}_+^2(248631579\Delta\kappa_- + 2245677353\kappa_+ + 17422730002)\right]\right\}$$

$$\frac{1}{\ell^7}\left\{-14\mathcal{E}^{3/2}[305\tilde{a}_-\Delta + 1607\tilde{a}_+]\right.$$
$$\left.+ \frac{\mathcal{E}^{5/2}[\nu(126497224\tilde{a}_-\Delta + 688003120\tilde{a}_+) - 253520875\tilde{a}_-\Delta - 998019442\tilde{a}_+]}{1050}\right\}$$

$$\frac{1}{\ell^8}\left\{\frac{7}{3}\mathcal{E}^{3/2}\left[\tilde{a}_-^2(1331\kappa_+ - 2578) + 2662\tilde{a}_-\tilde{a}_+\kappa_- + 1331\tilde{a}_+^2(\kappa_+ + 2)\right]\right.$$
$$+ \frac{\mathcal{E}^{5/2}}{4200}\left[\nu\left(-28\tilde{a}_-^2(14163997\kappa_+ + 7912369) - 793183832\tilde{a}_-\tilde{a}_+\kappa_- - 396591916\tilde{a}_+^2(\kappa_+ + 2)\right)\right.$$
$$+ 3\tilde{a}_-^2(24716321\Delta\kappa_- + 242351703\kappa_+ - 399754150)$$
$$+ 2\tilde{a}_-\tilde{a}_+(74148963\Delta\kappa_+ + 1186217480\Delta + 727055109\kappa_-)$$
$$\left.\left.+ \tilde{a}_+^2(74148963\Delta\kappa_- + 727055109\kappa_+ + 6340031818)\right]\right\}$$

$$\frac{1}{\ell^9}\left\{-\frac{42}{5}\sqrt{\mathcal{E}}[93\tilde{a}_-\Delta + 506\tilde{a}_+]\right.$$
$$\left.+ \frac{1}{840}\mathcal{E}^{3/2}[\nu(41837768\tilde{a}_-\Delta + 239782088\tilde{a}_+) - 101769441\tilde{a}_-\Delta - 423561642\tilde{a}_+]\right\}$$

$$\frac{1}{\ell^{10}}\left\{\frac{63}{10}\sqrt{\mathcal{E}}\left[\tilde{a}_-^2(88\kappa_+ - 171) + 176\tilde{a}_-\tilde{a}_+\kappa_- + 88\tilde{a}_+^2(\kappa_+ + 2)\right]\right.$$

$$+ \frac{\mathcal{E}^{3/2}}{3360}\left[\nu\left(-112\tilde{a}_-^2(1140621\kappa_+ + 1120396) - 255499104\tilde{a}_-\tilde{a}_+\kappa_- - 127749552\tilde{a}_+^2(\kappa_+ + 2)\right)\right.$$

$$+ \tilde{a}_-^2(26599377\Delta\kappa_- + 282234867\kappa_+ - 470833058)$$

$$+ 6\tilde{a}_-\tilde{a}_+(8866459\Delta\kappa_+ + 155168888\Delta + 94078289\kappa_-)$$

$$\left.\left.+\tilde{a}_+^2(26599377\Delta\kappa_- + 282234867\kappa_+ + 2627426630)\right]\right\}$$

$$\frac{1}{\ell^{11}}\left\{\frac{11}{560}\sqrt{\mathcal{E}}[\nu(387296\tilde{a}_-\Delta + 2308880\tilde{a}_+) - 1097925\tilde{a}_-\Delta - 4756668\tilde{a}_+]\right\}$$

$$\frac{1}{\ell^{12}}\left\{\frac{11\sqrt{\mathcal{E}}}{2240}\left[\nu\left(-112\tilde{a}_-^2(10347\kappa_+ + 14269) - 2317728\tilde{a}_-\tilde{a}_+\kappa_- - 1158864\tilde{a}_+^2(\kappa_+ + 2)\right)\right.\right.$$

$$+ \tilde{a}_-^2(262227\Delta\kappa_- + 2978061\kappa_+ - 5005550)$$

$$+ 6\tilde{a}_-\tilde{a}_+(87409\Delta\kappa_+ + 1644440\Delta + 992687\kappa_-)$$

$$\left.\left.+\tilde{a}_+^2(262227\Delta\kappa_- + 2978061\kappa_+ + 28885322)\right]\right\}$$

Something similar occurs for the angular momentum, where we find

$$\frac{\Delta J_{\text{ell}}(\ell, \tilde{a}_\pm, \mathcal{E})}{\pi G M^2 \nu^2} = \tag{5.21}$$

$$\frac{1}{\ell^3}\left\{-\frac{8}{15}\mathcal{E}^2[52\tilde{a}_-\Delta + 245\tilde{a}_+] + \frac{2}{15}\mathcal{E}^3[\nu(980\tilde{a}_-\Delta + 3680\tilde{a}_+) - 898\tilde{a}_-\Delta - 2159\tilde{a}_+]\right\}$$

$$+ \frac{1}{\ell^4}\left\{\frac{6}{5}\mathcal{E}^2\left[\tilde{a}_-^2(21\kappa_+ - 41) + 42\tilde{a}_-\tilde{a}_+\kappa_- + 21\tilde{a}_+^2(\kappa_+ + 2)\right]\right.$$

$$+ \frac{1}{70}\mathcal{E}^3\left[\nu\left(-28\tilde{a}_-^2(311\kappa_+ - 369) - 17416\tilde{a}_-\tilde{a}_+\kappa_- - 8708\tilde{a}_+^2(\kappa_+ + 2)\right)\right.$$

$$+ \tilde{a}_-^2(371\Delta\kappa_- + 9419\kappa_+ - 16514) + 2\tilde{a}_-\tilde{a}_+(371\Delta\kappa_+ + 7868\Delta + 9419\kappa_-)$$

$$\left.\left.+\tilde{a}_+^2(371\Delta\kappa_- + 9419\kappa_+ + 18530)\right]\right\}$$

$$+ \frac{1}{\ell^5}\left\{-\frac{8}{5}\mathcal{E}[95\tilde{a}_-\Delta + 468\tilde{a}_+] + \frac{1}{35}\mathcal{E}^2[\nu(55832\tilde{a}_-\Delta + 242872\tilde{a}_+) - 58346\tilde{a}_-\Delta - 166243\tilde{a}_+]\right\}$$

$$+ \frac{1}{\ell^6}\left\{6\mathcal{E}\left[\tilde{a}_-^2(20\kappa_+ - 39) + 40\tilde{a}_-\tilde{a}_+\kappa_- + 20\tilde{a}_+^2(\kappa_+ + 2)\right]\right.$$

$$+ \frac{1}{28}\mathcal{E}^2\left[\nu\left(-28\tilde{a}_-^2(1324\kappa_+ - 975) - 74144\tilde{a}_-\tilde{a}_+\kappa_- - 37072\tilde{a}_+^2(\kappa_+ + 2)\right)\right.$$

$$+ \tilde{a}_-^2(4319\Delta\kappa_- + 38618\kappa_+ - 64972) + 2\tilde{a}_-\tilde{a}_+(4319\Delta\kappa_+ + 49308\Delta + 38618\kappa_-)$$

$$\left.\left.+\tilde{a}_+^2(4319\Delta\kappa_- + 38618\kappa_+ + 190300)\right]\right\}$$

$$+ \frac{1}{\ell^7}\left\{-\frac{2}{3}[168\tilde{a}_-\Delta + 901\tilde{a}_+] + \frac{1}{6}\mathcal{E}[\nu(17536\tilde{a}_-\Delta + 88648\tilde{a}_+) - 26100\tilde{a}_-\Delta - 87115\tilde{a}_+]\right\}$$

$$
+ \frac{1}{\ell^8} \left\{ \frac{7}{2} \left[\tilde{a}_-^2 (23\kappa_+ - 45) + 46\tilde{a}_-\tilde{a}_+\kappa_- + 23\tilde{a}_+^2 (\kappa_+ + 2) \right] \right.
$$

$$
+ \frac{1}{24}\mathcal{E} \left[\nu \left(-56\tilde{a}_-^2 (961\kappa_+ - 154) - 107632\tilde{a}_-\tilde{a}_+\kappa_- - 53816\tilde{a}_+^2 (\kappa_+ + 2) \right) \right.
$$

$$
+ \tilde{a}_-^2 (8869\Delta\kappa_- + 74819\kappa_+ - 126006) + 2\tilde{a}_-\tilde{a}_+ (8869\Delta\kappa_+ + 113260\Delta + 74819\kappa_-)
$$

$$
\left. \left. + \tilde{a}_+^2 (8869\Delta\kappa_- + 74819\kappa_+ + 549338) \right] \right\}
$$

$$
+ \frac{1}{\ell^9} \left\{ \frac{1}{60} [\nu(74676\tilde{a}_-\Delta + 418432\tilde{a}_+) - 158892\tilde{a}_-\Delta - 615951\tilde{a}_+] \right\}
$$

$$
+ \frac{1}{\ell^{10}} \left\{ \frac{3}{80} \left[\nu \left(-112\tilde{a}_-^2 (216\kappa_+ + 115) - 48384\tilde{a}_-\tilde{a}_+\kappa_- - 24192\tilde{a}_+^2 (\kappa_+ + 2) \right) \right. \right.
$$

$$
+ \tilde{a}_-^2 (4921\Delta\kappa_- + 47168\kappa_+ - 80140) + 2\tilde{a}_-\tilde{a}_+ (4921\Delta\kappa_+ + 75348\Delta + 47168\kappa_-)
$$

$$
\left. \left. + \tilde{a}_+^2 (4921\Delta\kappa_- + 47168\kappa_+ + 416112) \right] \right\}
$$

On the other hand, after similar manipulations, we arrive at

$$
\Delta J_{\mathrm{hyp}}(\ell, \tilde{a}_\pm, \mathcal{E}) = + \frac{\Delta J_{\mathrm{ell}}(\ell, \tilde{a}_\pm, \mathcal{E})}{\pi} \cos^{-1}\left(\frac{-1}{e_N} \right) + \Delta J_{\mathrm{hyp}}^{(\mathrm{odd})}(\ell, \tilde{a}_\pm, \mathcal{E}), \qquad (5.22)
$$

where $\Delta J_{\mathrm{hyp}}^{(\mathrm{even})}$ is odd under $J \to -J$ (or $e \to -e$). Once again, since in this case ΔJ_{ell} is even under J-parity, the B2B correspondence in (3.11) applies.

The expression for the odd term is given by:

$$
\frac{\sqrt{2} e_N^4 \Delta J_{\mathrm{hyp}}^{(\mathrm{odd})}(\ell, \tilde{a}_\pm, \mathcal{E})}{GM^2\nu^2} = \qquad\qquad (5.23)
$$

$$
\ell^2 \left\{ -\frac{128}{5}\mathcal{E}^{9/2}[\tilde{a}_-\Delta + 7\tilde{a}_+] + \frac{32}{35}\mathcal{E}^{11/2}[\nu(63\tilde{a}_-\Delta + 357\tilde{a}_+) - 109\tilde{a}_-\Delta - 203\tilde{a}_+] \right\}
$$

$$
+ \ell \left\{ \frac{128}{5}\mathcal{E}^{9/2} \left[\tilde{a}_-^2 (\kappa_+ - 2) + 2\tilde{a}_-\tilde{a}_+\kappa_- + \tilde{a}_+^2 (\kappa_+ + 2) \right] \right.
$$

$$
- \frac{32}{35}\mathcal{E}^{11/2} \left[\nu \left(7\tilde{a}_-^2 (11\kappa_+ - 14) + 154\tilde{a}_-\tilde{a}_+\kappa_- + 77\tilde{a}_+^2 (\kappa_+ + 2) \right) \right.
$$

$$
\left. \left. + \tilde{a}_-^2 (232 - 123\kappa_+) - 2\tilde{a}_-\tilde{a}_+ (98\Delta + 123\kappa_-) - 3\tilde{a}_+^2 (41\kappa_+ + 12) \right] \right\}
$$

$$
+ \ell^0 \left\{ -\frac{32}{45}\mathcal{E}^{7/2}[978\tilde{a}_-\Delta + 4675\tilde{a}_+] \right.
$$

$$
\left. + \frac{8\mathcal{E}^{9/2}[\nu(1009106\tilde{a}_-\Delta + 4045202\tilde{a}_+) - 935472\tilde{a}_-\Delta - 2512391\tilde{a}_+]}{1575} \right\}
$$

$$
+ \frac{1}{\ell} \left\{ \frac{8}{15}\mathcal{E}^{7/2} \left[\tilde{a}_-^2 (1091\kappa_+ - 2127) + 2182\tilde{a}_-\tilde{a}_+\kappa_- + 1091\tilde{a}_+^2 (\kappa_+ + 2) \right] \right.
$$

$$
+ \frac{2\mathcal{E}^{9/2}}{1575} \left[\nu \left(-28\tilde{a}_-^2 (126061\kappa_+ - 121315) - 7059416\tilde{a}_-\tilde{a}_+\kappa_- - 3529708\tilde{a}_+^2 (\kappa_+ + 2) \right) \right.
$$

$$
+ \tilde{a}_-^2 (309449\Delta\kappa_- + 3479857\kappa_+ - 5918310) + 2\tilde{a}_-\tilde{a}_+ (309449\Delta\kappa_+ + 3785012\Delta + 3479857\kappa_-)
$$

$$
\left. \left. + \tilde{a}_+^2 (309449\Delta\kappa_- + 3479857\kappa_+ + 12238918) \right] \right\}
$$

$$+ \frac{1}{\ell^2}\Bigg\{ -\frac{16}{45}\mathcal{E}^{5/2}[4350\tilde{a}_-\Delta + 21983\tilde{a}_+]$$

$$\frac{16\mathcal{E}^{7/2}[\nu(2150743\tilde{a}_-\Delta + 10018946\tilde{a}_+) - 2626776\tilde{a}_-\Delta - 8039878\tilde{a}_+]}{1575}\Bigg\}$$

$$+ \frac{1}{\ell^3}\Bigg\{ \frac{4}{15}\mathcal{E}^{5/2}\left[\tilde{a}_-^2(4477\kappa_+ - 8739) + 8954\tilde{a}_-\tilde{a}_+\kappa_- + 4477\tilde{a}_+^2(\kappa_+ + 2)\right]$$

$$+ \frac{\mathcal{E}^{7/2}}{1575}\left[\nu\left(-28\tilde{a}_-^2(986447\kappa_+ - 501590) - 55241032\tilde{a}_-\tilde{a}_+\kappa_- - 27620516\tilde{a}_+^2(\kappa_+ + 2)\right)\right.$$

$$+ \tilde{a}_-^2(3765328\Delta\kappa_- + 32458829\kappa_+ - 54619230)$$

$$+ 2\tilde{a}_-\tilde{a}_+(3765328\Delta\kappa_+ + 45132304\Delta + 32458829\kappa_-)$$

$$\left.+\tilde{a}_+^2(3765328\Delta\kappa_- + 32458829\kappa_+ + 196050926)\right]\Bigg\}$$

$$+ \frac{1}{\ell^4}\Bigg\{ -\frac{8}{45}\mathcal{E}^{3/2}[5910\tilde{a}_-\Delta + 30949\tilde{a}_+]$$

$$+ \frac{4\mathcal{E}^{5/2}[\nu(11019148\tilde{a}_-\Delta + 55964216\tilde{a}_+) - 17180511\tilde{a}_-\Delta - 59099908\tilde{a}_+]}{1575}\Bigg\}$$

$$+ \frac{1}{\ell^5}\Bigg\{ \frac{2}{3}\mathcal{E}^{3/2}\left[\tilde{a}_-^2(1165\kappa_+ - 2277) + 2330\tilde{a}_-\tilde{a}_+\kappa_- + 1165\tilde{a}_+^2(\kappa_+ + 2)\right]$$

$$+ \frac{\mathcal{E}^{5/2}}{3150}\left[\nu\left(-28\tilde{a}_-^2(2415106\kappa_+ - 257035) - 135245936\tilde{a}_-\tilde{a}_+\kappa_- - 67622968\tilde{a}_+^2(\kappa_+ + 2)\right)\right.$$

$$+ \tilde{a}_-^2(11212334\Delta\kappa_- + 97928347\kappa_+ - 165264510)$$

$$+ 2\tilde{a}_-\tilde{a}_+(11212334\Delta\kappa_+ + 148172192\Delta + 97928347\kappa_-)$$

$$\left.+\tilde{a}_+^2(11212334\Delta\kappa_- + 97928347\kappa_+ + 733208698)\right]\Bigg\}$$

$$+ \frac{1}{\ell^6}\Bigg\{ -\frac{4}{3}\sqrt{\mathcal{E}}[168\tilde{a}_-\Delta + 901\tilde{a}_+]$$

$$+ \frac{4}{9}\mathcal{E}^{3/2}[\nu(31821\tilde{a}_-\Delta + 171094\tilde{a}_+) - 59298\tilde{a}_-\Delta - 219324\tilde{a}_+]\Bigg\}$$

$$+ \frac{1}{\ell^7}\Bigg\{ 7\sqrt{\mathcal{E}}\left[\tilde{a}_-^2(23\kappa_+ - 45) + 46\tilde{a}_-\tilde{a}_+\kappa_- + 23\tilde{a}_+^2(\kappa_+ + 2)\right]$$

$$+ \frac{1}{12}\mathcal{E}^{3/2}\left[\nu\left(-56\tilde{a}_-^2(2257\kappa_+ + 536) - 252784\tilde{a}_-\tilde{a}_+\kappa_- - 126392\tilde{a}_+^2(\kappa_+ + 2)\right)\right.$$

$$+ \tilde{a}_-^2(23632\Delta\kappa_- + 216323\kappa_+ - 366426) + 2\tilde{a}_-\tilde{a}_+(23632\Delta\kappa_+ + 339304\Delta + 216323\kappa_-)$$

$$\left.+\tilde{a}_+^2(23632\Delta\kappa_- + 216323\kappa_+ + 1797674)\right]\Bigg\}$$

$$+ \frac{1}{\ell^8}\Bigg\{ \frac{1}{30}\sqrt{\mathcal{E}}[\nu(74676\tilde{a}_-\Delta + 418432\tilde{a}_+) - 158892\tilde{a}_-\Delta - 615951\tilde{a}_+]\Bigg\}$$

$$+ \frac{1}{\ell^9}\Bigg\{ \frac{3}{40}\sqrt{\mathcal{E}}\left[\nu\left(-112\tilde{a}_-^2(216\kappa_+ + 115) - 48384\tilde{a}_-\tilde{a}_+\kappa_- - 24192\tilde{a}_+^2(\kappa_+ + 2)\right)\right.$$

$$+ \tilde{a}_-^2(4921\Delta\kappa_- + 47168\kappa_+ - 80140) + 2\tilde{a}_-\tilde{a}_+(4921\Delta\kappa_+ + 75348\Delta + 47168\kappa_-)$$

$$\left.+\tilde{a}_+^2(4921\Delta\kappa_- + 47168\kappa_+ + 416112)\right]\Bigg\}$$

Notice in both cases some of the terms in the hyperbolic result do not allow for a smooth

analytic continuation in the binding energy. However, all of these pieces nicely cancel out in the B2B dictionary of (3.9) or (3.11).

5.5 Local-in-time

We move on now onto the conservative sector and local-in-time effects. We concentrate on the 4PN dynamics which has been established by independent derivations [42–45, 52–55].[9]

Introducing the split between local- and non-local-in-time contributions,

$$\frac{\chi}{2} = \sum_{j=1}^{\infty} \frac{1}{j^n} \left(\chi^{(n)}_{j,\text{loc}}(v_\infty) + \chi^{(n)}_{j,\text{nloc}}(v_\infty) \right) , \tag{5.24}$$

where $v_\infty \equiv \sqrt{\gamma^2 - 1}$ serves as an expansion parameter, we have

$$\chi^{(1)}_{j,\text{loc}} = \frac{1}{v_\infty} + 2v_\infty ,$$

$$\chi^{(2)}_{j,\text{loc}} = \frac{3\pi}{2} + \left[\frac{15\pi}{8} - \frac{3\pi\nu}{4} \right] v_\infty^2 + \left[\frac{9\pi\nu^2}{16} - \frac{3\pi\nu}{4} \right] v_\infty^4 + \left[-\frac{15\pi\nu^3}{32} + \frac{27\pi\nu^2}{64} + \frac{9\pi\nu}{64} \right] v_\infty^6$$

$$\chi^{(3)}_{j,\text{loc}} = -\frac{1}{3v_\infty^3} + \frac{4}{v_\infty} + [24 - 8\nu]v_\infty + \left[8\nu^2 - 36\nu + \frac{64}{3} \right] v_\infty^3 + \left[-8\nu^3 + 34\nu^2 - \frac{91\nu}{5} \right] v_\infty^5$$

$$\chi^{(4)}_{j,\text{loc}} = \left[-\frac{15\pi\nu}{4} + \frac{105\pi}{8} \right] + \left[\frac{45\pi\nu^2}{8} + \left(\frac{123\pi^3}{256} - \frac{109\pi}{2} \right) \nu + \frac{315\pi}{8} \right] v_\infty^2$$

$$+ \left[-\frac{225\pi\nu^3}{32} - \frac{3}{512}\pi \left(123\pi^2 - 12872 \right) \nu^2 + \frac{\pi \left(100803\pi^2 - 5016832 \right) \nu}{49152} + \frac{3465\pi}{128} \right] v_\infty^4$$

$$\chi^{(5)}_{j,\text{loc}} = \frac{1}{5v_\infty^5} - \frac{2}{v_\infty^3} + \frac{32 - 8\nu}{v_\infty} + \left[24\nu^2 + \left(\frac{41\pi^2}{8} - \frac{1168}{3} \right) \nu + 320 \right] v_\infty$$

$$+ \left[-40\nu^3 + \left(\frac{7342}{9} - \frac{287\pi^2}{24} \right) \nu^2 + \left(\frac{5069\pi^2}{144} - \frac{227059}{135} \right) \nu + 640 \right] v_\infty^3 \tag{5.25}$$

---

[9]The conservative 5PN dynamics was recently reported in [59, 75], see also [33, 76–80], and partial values to 6PN order in [58, 60]. Despite some disagreements in the literature, notably for memory terms, we checked the B2B correspondence remains valid regardless of the specific values associated with local-in-time dynamics.

From here, and using the algebraic relations discussed in [1, 2], we find

$$
\begin{aligned}
\frac{f_1^{\mathrm{loc}}}{\Gamma} &= \frac{2}{v_\infty^2} + 4\,, \\
\frac{f_2^{\mathrm{loc}}}{\Gamma} &= \frac{6}{v_\infty^2} + \frac{15}{2}\,, \\
\frac{f_3^{\mathrm{loc}}}{\Gamma} &= \left[-5\nu + \frac{17}{2}\right]\frac{1}{v_\infty^2} + \left[\frac{3\nu^2}{4} - \frac{37\nu}{2} + 9\right] + \left[-\frac{3\nu^3}{8} + \frac{33\nu^2}{16} - \frac{471\nu}{80}\right]v_\infty^2 \\
\frac{f_4^{\mathrm{loc}}}{\Gamma} &= \left[\frac{7\nu^2}{2} + \left(\frac{41\pi^2}{32} - \frac{160}{3}\right)\nu + 8\right]\frac{1}{v_\infty^2} + \left[-\frac{5\nu^3}{4} + \frac{49\nu^2}{2} + \left(\frac{33601\pi^2}{6144} - \frac{3877}{45}\right)\nu + \frac{129}{16}\right] \\
\frac{f_5^{\mathrm{loc}}}{\Gamma} &= \left[-\frac{9\nu^3}{4} + \left(\frac{2579}{24} - \frac{205\pi^2}{64}\right)\nu^2 + \left(\frac{14173\pi^2}{6144} - \frac{3707}{360}\right)\nu + 6\right]\frac{1}{v_\infty^2}
\end{aligned}
\tag{5.26}
$$

for the f_i's in the expansion of the center-of-mass momentum in (2.2). These values capture all the needed information to 4PN order. For instance, the application of the B2B map requires the even coefficients of the scattering angle, which can be obtained directly from the f_i coefficients [1, 2]

$$
\chi_{j,\mathrm{loc}}^{(6)} = \frac{5\pi v_\infty^6}{16\Gamma^6}\left(\frac{f_2^3}{2} + 3f_1 f_3 f_2 + 3f_4 f_2 + \frac{3}{2}f_3^2 + \frac{3}{2}f_1^2 f_4 + 3f_1 f_5 + \frac{3f_6}{2}\right).
\tag{5.27}
$$

Due to the scaling $f_i \simeq 1/v_\infty^2$ [1, 2], the PN contribution from f_6 is subleading, such that

$$
\chi_{j,\mathrm{loc}}^{(6)} = \left[\frac{105\pi\nu^2}{16} + \frac{5}{256}\pi\left(123\pi^2 - 8000\right)\nu + \frac{1155\pi}{8}\right]
\tag{5.28}
$$
$$
+ \left[-\frac{525\pi\nu^3}{32} - \frac{5}{64}\pi\left(123\pi^2 - 7013\right)\nu^2 + \frac{\pi\left(771585\pi^2 - 37556864\right)\nu}{24576} + \frac{45045\pi}{64}\right]v_\infty^2 + \cdots
$$

which agrees with the known value to 4PN. The same reasoning applies to higher order terms. It is now straightforward to construct the (reduced) local-in-time bound radial action following the B2B dictionary, which takes the form

$$
i_r^{\mathrm{loc}} \equiv \frac{\mathcal{S}_{r,\mathrm{ell}}^{\mathrm{loc}}}{GM^2\nu} = \mathrm{sgn}(\hat{p}_\infty)\chi_j^{(1)} - j\left(1 + \frac{2}{\pi}\sum_{n=1}^{\infty}\frac{\chi_{j,\mathrm{loc}}^{(2n)}}{(1-2n)j^{2n}}\right),
\tag{5.29}
$$

with the 4PN contribution to the $\chi_{j,\mathrm{loc}}^{(2n)}$'s, up to $n = 4$, obtained from the f_i's. Using [1, 2]

$$
v_\infty^2 \to \left(1 + \mathcal{E} + \frac{\nu\mathcal{E}^2}{2}\right)^2 - 1\,,
\tag{5.30}
$$

the bound radial action then becomes a function of the (negative) binding energy after analytic continuation. From the radial action we compute all the local-in-time observables for bound

orbits through derivatives w.r.t. the angular momentum and binding energy. For example, we derived the local correction to the periastron advance to 4PN via

$$1 + \frac{\Delta\Phi_{\text{loc}}}{2\pi} = -\frac{\partial}{\partial j} i_r^{\text{loc}} , \qquad (5.31)$$

also directly from the value of the scattering angle using (2.8), yielding perfect agreement with the result reported in [81]. The map can also be shown to hold for known values at higher PN orders. For example, the bound radial action constructed through (5.26) neatly reproduces all the values presented in TABLE XIV of [58]. Furthermore, the B2B map between angle and periastron advanced was also used in the recent results at 5PN in [59].

5.6 Large-J expansion

Here we explicitly check the validity of the B2B dictionary in the large-eccentricity limit for the paradigmatic example at 4PN order. To evaluate the non-local dynamics will we use a (comprehensive) parameterization of the Newtonian orbit,

$$r = \frac{j^2}{1 + e \cos\alpha} , \qquad (5.32a)$$

$$\phi - \phi_0 = \alpha , \qquad (5.32b)$$

$$j^{-3}(t - t_0) = \frac{2}{(1 - e^2)^{3/2}} \arctan\left(\sqrt{\frac{1 - e}{1 + e}} \tan\frac{\alpha}{2}\right) - \frac{e}{1 - e^2} \frac{\sin\alpha}{1 + e \cos\alpha} , \qquad (5.32c)$$

$$\frac{dr}{dt} = \frac{e \sin\alpha}{j} , \qquad (5.32d)$$

$$\frac{d\phi}{dt} = \frac{(1 + e \cos\alpha)^2}{j^3} . \qquad (5.32e)$$

After rescaling the time parameter $\tau \equiv \frac{t}{GM}$, the non-local Hamiltonian defined in (4.22) may be written as

$$H_{\text{nloc}}(\tau) = H_{\text{tail}} + H_{\log r} , \qquad (5.33)$$

with[10]

$$H_{\text{tail}} = -\frac{M\nu^2}{15j^{10}} \text{Pf}_T \int \frac{d\tau'}{|\tau' - \tau|} F(\tau, \tau') \qquad (5.34)$$

$$H_{\log r} = -\frac{4M\nu^2}{15j^{10}} F(\tau, \tau) \log(r^2/T^2) , \qquad (5.35)$$

where Pf_T stands for *partie finie*, and at leading PN order we have [58, 60]

$$F(\tau, \tau') = (1 + e \cos\alpha)^2 (1 + e \cos\alpha')^2 (F_0 + e F_1 + e^2 F_2) , \qquad (5.36)$$

---

[10]The factor of $\log T$ is equivalent to the $\log(2e^{\gamma_E}\mu)$ in frequency space, see e.g. [42].

where

$$F_0 = 24 \, \cos(2\alpha - 2\alpha'), \tag{5.37}$$

$$F_1 = 9 \, \cos(2\alpha - 3\alpha') + 15 \, \cos(\alpha - 2\alpha') + 9 \, \cos(3\alpha - 2\alpha') + 15 \, \cos(2\alpha - \alpha'),$$

$$F_2 = -\frac{1}{4} \, \cos(\alpha + \alpha') + \frac{45}{8} \, \cos(3\alpha - \alpha') + \frac{45}{8} \, \cos(-3\alpha' + \alpha) \tag{5.38}$$

$$+ \frac{27}{8} \, \cos(3\alpha - 3\alpha') + \frac{77}{8} \, \cos(\alpha - \alpha'),$$

with $\alpha \equiv \alpha(\tau)$ and $\alpha' \equiv \alpha(\tau')$. The non-local radial action is then obtained by integrating over the orbit,

$$\mathcal{S}_r^{\mathrm{nloc}} = -\frac{GM}{2\pi} \int_{-a}^{a} d\alpha \frac{d\tau}{d\alpha} \big(H_{\mathrm{tail}} + H_{\log r}\big) \equiv \mathcal{S}_r^{\mathrm{tail}} + \mathcal{S}_r^{\log r}, \tag{5.39}$$

where the limits of integration given by hyperbolic-like ($a = \pi$) and elliptic-like ($a = \pi/2$) motion at leading order in $1/j$, respectively. Performing the (regularized) time and orbital integration we find

$$\frac{\mathcal{S}_{r,\mathrm{ell}}^{\mathrm{tail}}}{GM^2\nu} = 2\frac{\mathcal{S}_{r,\mathrm{hyp}}^{\mathrm{tail}}}{GM^2\nu} = -\frac{1}{2\pi}\frac{16\pi\mathcal{E}^2\nu}{15j^3}\left(37\log\left(\frac{|\mathcal{E}|T}{2j}\right) + 100\right), \qquad \text{(large-}e\text{ approx.)}$$

$$\frac{\mathcal{S}_{r,\mathrm{ell}}^{\log r}}{GM^2\nu} = 2\frac{\mathcal{S}_{r,\mathrm{hyp}}^{\log r}}{GM^2\nu} = -\frac{1}{2\pi}\frac{16\pi\,\nu\,\mathcal{E}^2}{15j^3}\left(37\ \log\left(\frac{\sqrt{2}j}{T\,\sqrt{|\mathcal{E}|}}\right) - \frac{85}{4}\right), \tag{5.40}$$

for each individual term, such that the sum becomes

$$\frac{\mathcal{S}_{r,\mathrm{ell}}^{\mathrm{nloc}}}{GM^2\nu} = 2\frac{\mathcal{S}_{r,\mathrm{hyp}}^{\mathrm{nloc}}}{GM^2\nu} = -\frac{1}{2\pi}\frac{16\pi\mathcal{E}^2\nu}{15j^3}\left(37\log\left(\frac{\sqrt{|\mathcal{E}|}}{\sqrt{2}}\right) + \frac{315}{4}\right), \qquad \text{(large-}e\text{ approx.)} \tag{5.41}$$

which, at this order, formally obeys the B2B correspondence in (4.25). However, while the expansion of the radial actions in the limit of large angular momentum may be related through the B2B map, the non-local contributions obtained in this fashion do not fully describe generic bound orbits. Nevertheless, similarly to the local-in-time effects, we find the B2B dictionary correctly captures all the logarithms of the binding energy.

5.7 Logarithms

Let us consider now the logarithms (in binding energy) resulting from the non-local-in-time dynamics described by the universal contribution in (4.22). As we mentioned earlier, the result takes the form,

$$\chi_{j,\mathrm{nloc}}^{(n)} = \chi_{j,\log}^{(n)} \log v_\infty + \cdots, \tag{5.42}$$

which starts at 4PN order, and has been computed to 6PN in [58],[11]

$$
\frac{\chi_{j,\log}^{(4)}}{\pi\nu} = -\frac{37v_\infty^4}{5} + \left[\frac{111\nu}{10} - \frac{1357}{280}\right]v_\infty^6 + \left[-\frac{111\nu^2}{8} + \frac{2517\nu}{560} - \frac{27953}{3360}\right]v_\infty^8 + \cdots ,
$$

$$
\frac{\chi_{j,\log}^{(5)}}{\nu} = -\frac{6272v_\infty^3}{45} + \left[\frac{13952\nu}{45} - \frac{74432}{525}\right]v_\infty^5 - \left[\frac{21632\nu^2}{45} - \frac{288224\nu}{1575} + \frac{881392}{11025}\right]v_\infty^7 + \cdots ,
$$

$$
\frac{\chi_{j,\log}^{(6)}}{\pi\nu} = -122v_\infty^2 + \left[\frac{811\nu}{2} - \frac{13831}{56}\right]v_\infty^4 + \left[-785\nu^2 + \frac{75595\nu}{168} + \frac{64579}{1008}\right]v_\infty^6 + \cdots ,
$$

$$
\frac{\chi_{j,\log}^{(7)}}{\nu} = -\frac{9344v_\infty}{15} + \left[\frac{48256\nu}{15} - \frac{284224}{105}\right]v_\infty^3 + \left[-\frac{118912\nu^2}{15} + \frac{11456416\nu}{1575} + \frac{587984}{567}\right]v_\infty^5 + \cdots ,
$$

$$
\frac{\chi_{j,\log}^{(8)}}{\pi\nu} = -\frac{595}{3} + \left[-\frac{15813}{8} + \frac{10535}{6}\nu\right]v_\infty^2 + \cdots
$$

$$(5.43)$$

More recently, the logarithmic contribution to the scattering angle have been obtained at 4PM, to all orders in the PN expansion [26, 27]. The result reads

$$
\frac{\chi_{j,\log}^{(4)}}{\nu\pi} = \frac{E}{M^2\nu^2\pi}\frac{\partial}{\partial j}\Delta E_{\text{hyp}}(j,\mathcal{E}) = \frac{2v_\infty^4}{\Gamma^3}\chi_{2\epsilon}(\gamma) , \tag{5.44}
$$

with the explicit expression for $\chi_{2\epsilon}(\gamma)$ given in [26, 27]. Performing a PN expansion we find,

$$
\frac{\chi_{j,\log}^{(4)}}{\nu\pi} = -\frac{37v_\infty^4}{5} + \left(\frac{111\nu}{10} - \frac{1357}{280}\right)v_\infty^6 + \left(-\frac{111\nu^2}{8} + \frac{2517\nu}{560} - \frac{27953}{3360}\right)v_\infty^8
$$
$$
+ \left(\frac{259\nu^3}{16} - \frac{963\nu^2}{448} + \frac{2699\nu}{224} + \frac{676273}{118272}\right)v_\infty^{10} + \cdots , \tag{5.45}
$$

which neatly agrees with the PN derivations, and we added the first new result at 7PN order. Due to the lack of information at higher PM orders, we will not consider this correction in what follows.

The Firsov representation can now be augmented to include the logarithmic corrections to describe generic orbits, re-written as

$$
\boldsymbol{p}^2 = p_\infty^2\left[1 + \sum_i \left(f_i^{\text{loc}} + f_i^{\text{log}}\log|v_\infty|\right)\left(\frac{GM}{r}\right)^i\right] . \tag{5.46}
$$

Notice that, as advertised, the factor of $\log r$ from potential-only contributions is traded by a logarithm of the binding energy in the full dynamics. Following the same steps as before we

---

[11]Except for $\chi_{j,\log}^{(8)}$, which we have obtained here through the Firsov representation.

arrive at

$$
\begin{aligned}
\frac{f_4^{\log}}{\Gamma} &= -\frac{296\nu}{15} - \frac{1357\nu v_\infty^2}{105} - \frac{27953\nu v_\infty^4}{1260} + \cdots, \\
\frac{f_5^{\log}}{\Gamma} &= -\frac{136\nu}{3v_\infty^2} + \left[\frac{796\nu^2}{15} + \frac{1271\nu}{25}\right] + \left[-\frac{37\nu^3}{5} + \frac{50441\nu^2}{1050} + \frac{412281\nu}{4900}\right] v_\infty^2 + \cdots, \\
\frac{f_6^{\log}}{\Gamma} &= \left[\frac{2576\nu^2}{15} + \frac{5916\nu}{25}\right]\frac{1}{v_\infty^2} - \left[\frac{496\nu^3}{5} + \frac{453982\nu^2}{1575} - \frac{15073564\nu}{33075}\right] + \cdots, \\
\frac{f_7^{\log}}{\Gamma} &= \left[-348\nu^3 - \frac{157946\nu^2}{105} + \frac{444883\nu}{19845}\right]\frac{1}{v_\infty^2} + \cdots,
\end{aligned}
\tag{5.47}
$$

for the logarithmic contributions in the expansion of the center-of-mass momentum. Momentarily, we will show how the above coefficient reproduce the correct logarithmic contributions to the binding energy for quasi-circular orbits through the B2B dictionary.

5.8 Large-eccentricity vs circular orbits

In order to evaluate how well the bound radial action for generic orbits can be approximated by the B2B map from the scattering angle obtained in a large-eccentricity expansion, we consider next a paradigmatic example: the binding energy for circular orbits. Although, as we shall see, the B2B map does not reproduce to the exact value in the literature [42–45, 54, 55], we find that several contributions, notably local-in-time effects and leading tail logarithms, do transition smoothly between unbound and bound motion.

We start by constructing the B2B radial action from the knowledge of the total scattering angle,

$$
i_r^{\text{large-}e} = \text{sgn}(\hat{p}_\infty)\chi_j^{(1)} - j\left(1 + \frac{2}{\pi}\sum_{n=1}^{\infty}\frac{\chi_{j,\text{loc}}^{(2n)} + \chi_{j,\text{nloc}}^{(2n)}}{(1-2n)j^{2n}}\right),
\tag{5.48}
$$

including non-local-in-time effects,[12] e.g. [58]

$$
\begin{aligned}
\frac{\chi_{j,\text{nloc}}^{(4)}}{\pi\nu} &= \left[-\frac{37}{5}\log v_\infty + \frac{37}{5}\log 2 - \frac{63}{4}\right]v_\infty^4 + \cdots, \\
\frac{\chi_{j,\text{nloc}}^{(6)}}{\pi\nu} &= \left[-122\log v_\infty + 122\log 2 - \frac{99}{8}(21\zeta_3 + 2)\right]v_\infty^2 + \cdots.
\end{aligned}
\tag{5.50}
$$

---

[12]In principle, to calculate the binding energy to 4PN from the radial action we need the value of $\chi_j^{(8)}$, which unfortunately is not presently known. Although we do not expect the Firsov representation to be valid for (non-logarithmic) non-local-in-time terms, we can still use it as a proxy for the full value. Hence, from

$$
\begin{aligned}
\chi_j^{(8)} = \frac{35\pi p_\infty^8}{256\nu^8 M^8}\Big(&f_2^4 + 12\left(f_1 f_3 + f_4\right)f_2^2 + 12\left(f_4 f_1^2 + 2f_5 f_1 + f_3^2 + f_6\right)f_2 + 6f_4^2 \\
&+4f_1^3 f_5 + 12f_3 f_5 + 6f_1^2\left(f_3^2 + 2f_6\right) + 12f_1\left(2f_3 f_4 + f_7\right) + 4f_8\Big),
\end{aligned}
\tag{5.49}
$$

truncated to 4PN order, we complete the expression in (5.48).

The binding energy is then extracted by imposing the vanishing of the radial action to solve for the angular momentum as a function of binding energy, and subsequently using the first-law of binary dynamics [82] to write $\mathcal{E}$ as a function of the orbital frequency through the parameter $x \equiv (GM\Omega)^{2/3}$. To 4PN order we find (recall $\epsilon = -2\mathcal{E}$)

$$
\epsilon(x) = \left\{ 1 + \left[-\frac{\nu}{12} - \frac{3}{4} \right] x + \left[-\frac{\nu^2}{24} + \frac{19\nu}{8} - \frac{27}{8} \right] x^2 \qquad \text{(large-e approx.)} \right.
$$
$$
+ \left[-\frac{35\nu^3}{5184} - \frac{155\nu^2}{96} - \frac{5}{576} \left(246\pi^2 - 6889 \right) \nu - \frac{675}{64} \right] x^3
$$
$$
+ \left[\frac{77\nu^4}{31104} + \frac{301\nu^3}{1728} + \frac{7 \left(2706\pi^2 - 71207 \right) \nu^2}{3456} + \frac{7 \left(19365\pi^2 - 98756 \right) \nu}{23040} - \frac{3969}{128} \right.
$$
$$
\left. \left. + \left(\frac{448 \log x}{15} - \frac{271768\zeta_3}{45} + \frac{19576}{135} + \frac{463232 \log 2}{45} \right) \nu \right] x^4 \right\} + \cdots .
$$
(5.51)

For illustrative purposes we have colored here only the contribution from the non-local term, which enters at $\mathcal{O}(\nu)$.

After direct comparison with the literature we find that all of the local-in-time contribution (and logarithms) perfectly matches the correct value for circular orbits. However, other terms, due to non-local effects, do not agree. At the end of the day there is a non-negligible mismatch,

$$
\delta\epsilon = \nu x^5 \frac{56}{135} \left(14559\,\zeta_3 - 329 + 144\gamma_E - 24528 \log 2 \right) \simeq 10^2\,\nu x^5 ,
$$
(5.52)

between the correct result at this order and the one obtained from the B2B map using a large-eccentricity approximation. This feature (including the presence of different transcendental numbers!) remains essentially unaltered at higher PN orders: contribution from local-in-time effects transition smoothly to the correct result for generic orbits, whereas the numerical values for most of the non-local corrections translated from a large-eccentricity expansion through the B2B dictionary do not capture the circular case.

The situation, however, is remarkably different for the logarithmic terms. Using the expressions in (5.43), or directly from the Firsov representation and the coefficients in (5.47), we obtain the following contribution to the bound radial action to 6PN through the B2B map,

$$
i_r^{\log} = \frac{2}{\pi} \sum_{n=2}^{n=4} \frac{\chi_{j,\log}^{(2n)}}{(1 - 2n)j^{2n}} + \cdots .
$$
(5.53)

Performing the same manipulations as before, we find

$$
\begin{aligned}
\epsilon_{\log x} = \Bigg\{ & \frac{448}{15}\nu x^5 + \left[\left(-\frac{224}{5} - \frac{432}{5} \right) \nu^2 + \left(-176 + \frac{1172}{35} \right) \nu \right] x^6 \qquad \text{(large-e approx.)} \\
& + \left[\left(\frac{616}{27} + \frac{792}{5} + \frac{176}{3} \right) \nu^3 + \left(\frac{39776}{45} + \frac{491326}{315} - \frac{1394492}{945} \right) \nu^2 \right. \\
& \left. + \left(-\frac{2638064}{45} + \frac{6032774}{105} + \frac{1138874}{1215} \right) \nu \right] x^7 \Bigg\} \log x \,,
\end{aligned}
$$
(5.54)

for the logarithmic contribution to the binding energy obtained via scattering data to 6PN order. (Notice this included different orders in the $1/j$ expansion of the scattering angle.) After adding them all up, they beautifully reproduce the correct value for circular orbits. This demonstrates the validity of the B2B map and Firsov representation both for local-in-time as well as (leading) tail logarithms for generic orbits.

6 Discussion

In this paper we have extended the B2B correspondence to include radiation effects, both in the dissipative and conservative sectors. We have found various types of analytic continuations between radiative observables for unbound and bound orbits,

$$
\Delta \mathcal{O}_{\text{ell}}(J, \mathcal{E}) = \Delta \mathcal{O}_{\text{hyp}}(J, \mathcal{E}) - \sigma_{\mathcal{O}} \Delta \mathcal{O}_{\text{hyp}}(-J, \mathcal{E}) \,,
$$

notably for the total (source) energy and angular momentum with $\sigma_{E/J} = +/-$, respectively; as well as conservative radiation-reaction contributions to the radial action,

$$
\mathcal{S}_{r,\text{ell}}(J) = \mathcal{S}_{r,\text{hyp}}(J) - \mathcal{S}_{r,\text{hyp}}(-J) \,,
$$

in the large-eccentricity limit. While the latter encapsulates all the local-in-time terms as well as the non-local-in-time logarithmic corrections, other non-local contributions in generic bound states are not captured by the large J expansion. This is easy to see already from the expression in (4.22). Assuming the validity of the adiabatic approximation, we can evaluate the integral over the conservative trajectory. Hence, performing a change of variables, e.g. $u \equiv \omega \, e a^{3/2}$, with (e, a) the orbital elements [58, 60], as well as using the parameterized form for the trajectory in terms of v, the 'eccentric anomaly,'

$$
r_{\text{ell}}(v) = a(1 - e \cos v) \,, \qquad r_{\text{hyp}}(v) = a(e \cosh v - 1) \,,
$$

we can readily factor out the tail logarithms out of the integral, yielding a contribution to the radial action proportional to[13]

$$
S^{\log}_{r,\text{ell/hyp}} \propto \Delta E_{\text{ell/hyp}} \log |\mathcal{E}| \,.
$$

---

[13] More generally, within the realm of the PM expansion, this is due to the fact that the pole from radiation modes in the tail effect is accompanied by a factor of $v_\infty^{-2(d-4)}$. The latter is ultimately responsible for the $\log v_\infty$ in the effective action [26, 27]. Hence, the universal character of the divergent part of the tail implies that both appear multiplied by the total radiated energy at the end of the day, see §4.5.

As a result of the B2B map for the total radiated energy, this implies the B2B correspondence for the logarithmic terms in the conservative sector. However, the result also features left-over integrals of the sort (schematically)

$$\int_{\text{ell}} F(u) \log u \, du \qquad \text{vs} \qquad \int_{\text{hyp}} F(u) \log u \, du \,,$$

with $F(u)$ the (dimensionless) energy flux, see e.g. [58, 60] for examples in the PN context. As discussed in detail in [58, 60], the presence of the $\log u$ produces wildly different values depending on the trajectory, involving even different types of transcendental numbers. For instance, while the quasi-circular binding energy features a factor of γ_E at 4PN, the scattering angle does not. This precludes the existence of a straightforward map at the level of the final answer which would connect generic non-local-in-time contributions from the above integral evaluated on unbound and bound orbits.

It is possible, however, to establish a relationship at the level of the integrand. As it is well known, e.g. [83], we can obtain the radial motion for elliptic-like orbits from hyperbolic-like motion directly via analytic continuation to negative binding energy and complex eccentric anomaly. Hence, we can search for the existence of an analytic continuation prior to performing the integration. For instance, on the one hand we find the hyperbolic result for the non-local-in time term at leading PN order leads to the integral

$$\int_0^\infty dp \, p^6 |I^{ij}_{\text{hyp}}(p)|^2 \log \left(p \, \Omega_{\text{hyp}} \right) \,,$$

where we made a change of variables $p \equiv \omega/\Omega_{\text{hyp}}$, and introduced a fictitious 'orbital frequency' $\Omega_{\text{hyp}} \equiv (2\mathcal{E})^{3/2}/GM$. Notice the parameter p is a continuous variable in this case. The leading quadrupolar flux is given by $|I^{ij}_{\text{hyp}}(p)|^2 = |\hat{I}^{ij}_{\text{hyp}}(ip)|^2$, as an analytic continuation of the following function,

$$|\hat{I}^{ij}_{\text{hyp}}(p)|^2 = -\frac{8 \, G^4 \, M^6 \, \pi^2 \, a^4 \, \nu^2}{3 \, e^4 \, p^4} \left[3e^2 \left(1 - e^2 \right) \left(1 + \left(1 - e^2 \right) p^2 \right) H^{(1)}_{p-1}(ep)^2 \right.$$
$$- 3e \left(1 - e^2 \right) \left(-e^2 p(2p+3) + 2(p+1)^2 \right) H^{(1)}_p(ep) H^{(1)}_{p-1}(ep)$$
$$\left. + \left(-3e^6 p^2 + e^4 \left(12p^2 + 9p + 1 \right) - 3e^2(p+1)(5p+2) + 6(p+1)^2 \right) H^{(1)}_p(ep)^2 \right] \,,$$

with (e, a) the orbital elements. The Hankel function is given by

$$H^{(1)}_p(x) = \frac{1}{i\pi} \int_{-\infty}^{+\infty} dv \, e^{x \sinh v - pv} \,,$$

which turns into the familiar $K_p(x)$ Bessel function after analytic continuation $x \to -ix$.

On the other hand, the elliptic case involves a sum over harmonics of the type [66]

$$\sum_{p=1}^\infty p^6 |I^{ij}_{\text{ell}}(p)|^2 \log \left(p \, \Omega_{\text{ell}} \right) \,,$$

with $\Omega_{\mathrm{ell}} \equiv (-2\mathcal{E})^{3/2}/GM$ the true frequency of circular orbits (which may be obtained directly from Ω_{hyp} via analytic continuation in $\mathcal{E}$), and the quadrupole flux

$$
\begin{aligned}
|I_{\mathrm{ell}}^{ij}(p)|^2 = \frac{8\,G^4\,M^6\,a^4\,\nu^2}{3\,e^4\,p^4}\Bigg[& 3e^2\left(1-e^2\right)\left(1+\left(1-e^2\right)p^2\right)J_{p-1}(ep)^2 \\
& -3e\left(1-e^2\right)\left(-e^2 p(2p+3)+2(p+1)^2\right)J_p(ep)J_{p-1}(ep) \\
& +\left(-3e^6 p^2 + e^4\left(12p^2+9p+1\right)-3e^2(p+1)(5p+2)+6(p+1)^2\right)J_p(ep)^2\Bigg],
\end{aligned}
$$

which is written in terms of the following Bessel function

$$
J_p(x) = \frac{1}{2\pi}\int_{-\pi}^{+\pi} dv\, e^{i(x\sin v - pv)}\,.
$$

The reader will immediately notice the resemblance between the two expressions. In particular, the analytic continuation in $p \to ip$ of the hyperbolic result plus the replacement $H_p^{(1)} \to J_p$ leads to the integrand, albeit with a discrete variable, for elliptic-like motion. Furthermore, the latter replacement between Bessel functions can be understood as the analytic continuation in $v \to iv$ associated with the link between unbound and bound (periodic) parameterizations of the orbit. From here we conclude that, indeed, we can find an analytic continuation at the level of the integrands. Yet, it is also clear the relationship ceases to apply once we expand in small/large eccentricity limits. As a consequence, other than the results uncovered here, it seems unlikely that a B2B-type map can connect non-local-in-time scattering data to generic bound orbits. It is still unclear, however, whether bound states with non-negligible eccentricities may be well approximated by the original B2B dictionary. We will explore this in more detail in future work.

We have concentrated here on local- and non-local-in-time tail effects. For the sake of completeness, let us conclude with a few comments regarding non-linear conservative memory terms, which are expected to be indistinguishable from other local-in-time effects and therefore readily incorporated in the B2B dictionary. The leading memory contribution may be computed through the same topology as in Fig. 3 (but including the quadrupole coupling and the full radiative field in the middle line instead of the monopole term and quasi-static potential). Similarly to tail terms, the separation between dissipative and conservative effects must be performed at the level of the full equations of motion, which may be derived using the Keldysh-Schwinger formalism [52, 84, 85]. Yet, at the 5PN order at which radiation-reaction memory corrections start to contribute, we also encounter other non-linear dissipative effects correcting the leading (Burke-Thorne) back-reaction force. The additional terms may be obtained via the EFT approach by including the (seagull-type) non-linear worldline coupling between the binary's quadrupole and the curvature tensor, see e.g. [59, 86].[14] As it turns out,

---

[14]These should not be confused with effects that enter the dynamics at quadratic order in the leading back-reaction force. In the PM EFT language of [22], the latter arise through iterations involving the deflection due to the leading dissipative effects inserted into the tree-level radiation-reaction effective action.

the extra terms also entail three quadrupole moments and an even number of time derivatives, as in the memory contribution. Therefore, they can mimic the scaling of time-symmetric conservative effects. Furthermore, total time derivatives (known as 'Schott terms') may not only be present in the balance equations, they may also remain once averaged over the orbital motion. Hence, one must exercise special care when separating the various pieces entering the dynamics through the product of (more than two) multipole moments. Although yielding somewhat subtle effects, all the conservative memory terms are purely local in time, and therefore are automatically included in the original B2B dictionary. We will discuss these contributions elsewhere.

Acknowledgments

Note added: While the results of this project were prepared for submission, the work of [87] appeared which has some overlap with the analysis in §3.1-§3.3 restricted to the case of spin-independent effects.

References

[1] G. Kälin and R. A. Porto, *From Boundary Data to Bound States*, *JHEP* **01** (2020) 072 [1910.03008].

[2] G. Kälin and R. A. Porto, *From boundary data to bound states. Part II: Scattering angle to dynamical invariants (with twist)*, *JHEP* **02** (2020) 120 [1911.09130].

[3] C. Cheung, I. Z. Rothstein and M. P. Solon, *From Scattering Amplitudes to Classical Potentials in the Post-Minkowskian Expansion*, *Phys. Rev. Lett.* **121** (2018) 251101 [1808.02489].

[4] A. Guevara, A. Ochirov and J. Vines, *Scattering of Spinning Black Holes from Exponentiated Soft Factors*, *JHEP* **09** (2019) 056 [1812.06895].

[5] D. A. Kosower, B. Maybee and D. O'Connell, *Amplitudes, Observables, and Classical Scattering*, *JHEP* **02** (2019) 137 [1811.10950].

[6] B. Maybee, D. O'Connell and J. Vines, *Observables and amplitudes for spinning particles and black holes*, *JHEP* **12** (2019) 156 [1906.09260].

---

[15]https://www.youtube.com/watch?v=WZ7MEYjvT8s&t=40s

[7] N. E. J. Bjerrum-Bohr, P. H. Damgaard, G. Festuccia, L. Plante and P. Vanhove, *General Relativity from Scattering Amplitudes*, *Phys. Rev. Lett.* **121** (2018) 171601 [1806.04920].

[8] Z. Bern, C. Cheung, R. Roiban, C.-H. Shen, M. P. Solon and M. Zeng, *Scattering Amplitudes and the Conservative Hamiltonian for Binary Systems at Third Post-Minkowskian Order*, *Phys. Rev. Lett.* **122** (2019) 201603 [1901.04424].

[9] Z. Bern, C. Cheung, R. Roiban, C.-H. Shen, M. P. Solon and M. Zeng, *Black Hole Binary Dynamics from the Double Copy and Effective Theory*, *JHEP* **10** (2019) 206 [1908.01493].

[10] Z. Bern, A. Luna, R. Roiban, C.-H. Shen and M. Zeng, *Spinning Black Hole Binary Dynamics, Scattering Amplitudes and Effective Field Theory*, 2005.03071.

[11] C. Cheung and M. P. Solon, *Tidal Effects in the Post-Minkowskian Expansion*, *Phys. Rev. Lett.* **125** (2020) 191601 [2006.06665].

[12] M.-Z. Chung, Y.-t. Huang, J.-W. Kim and S. Lee, *Complete Hamiltonian for spinning binary systems at first post-Minkowskian order*, 2003.06600.

[13] D. Kosmopoulos and A. Luna, *Quadratic-in-Spin Hamiltonian at $\mathcal{O}(G^2)$ from Scattering Amplitudes*, 2102.10137.

[14] Z. Bern, J. Parra-Martinez, R. Roiban, M. S. Ruf, C.-H. Shen, M. P. Solon et al., *Scattering Amplitudes and Conservative Binary Dynamics at $\mathcal{O}(G^4)$*, *Phys. Rev. Lett.* **126** (2021) 171601 [2101.07254].

[15] P. Di Vecchia, C. Heissenberg, R. Russo and G. Veneziano, *The Eikonal Approach to Gravitational Scattering and Radiation at $\mathcal{O}(G^3)$*, 2104.03256.

[16] A. Cristofoli, R. Gonzo, D. A. Kosower and D. O'Connell, *Waveforms from Amplitudes*, 2107.10193.

[17] E. Herrmann, J. Parra-Martinez, M. S. Ruf and M. Zeng, *Gravitational Bremsstrahlung from Reverse Unitarity*, *Phys. Rev. Lett.* **126** (2021) 201602 [2101.07255].

[18] Y. F. Bautista and N. Siemonsen, *Post-Newtonian Waveforms from Spinning Scattering Amplitudes*, 2110.12537.

[19] T. Damour, *Gravitational scattering, post-Minkowskian approximation and Effective One-Body theory*, *Phys. Rev. D* **94** (2016) 104015 [1609.00354].

[20] W. D. Goldberger and A. K. Ridgway, *Radiation and the classical double copy for color charges*, *Phys. Rev. D* **95** (2017) 125010 [1611.03493].

[21] T. Damour, *Classical and quantum scattering in post-Minkowskian gravity*, *Phys. Rev. D* **102** (2020) 024060 [1912.02139].

[22] G. Kälin and R. A. Porto, *Post-Minkowskian Effective Field Theory for Conservative Binary Dynamics*, *JHEP* **11** (2020) 106 [2006.01184].

[23] G. Kälin, Z. Liu and R. A. Porto, *Conservative Dynamics of Binary Systems to Third Post-Minkowskian Order from the Effective Field Theory Approach*, *Phys. Rev. Lett.* **125** (2020) 261103 [2007.04977].

[24] G. Kälin, Z. Liu and R. A. Porto, *Conservative Tidal Effects in Compact Binary Systems to Next-to-Leading Post-Minkowskian Order*, *Phys. Rev. D* **102** (2020) 124025 [2008.06047].

[25] Z. Liu, R. A. Porto and Z. Yang, *Spin Effects in the Effective Field Theory Approach to Post-Minkowskian Conservative Dynamics*, *JHEP* **06** (2021) 012 [`2102.10059`].

[26] C. Dlapa, G. Kälin, Z. Liu and R. A. Porto, *Dynamics of Binary Systems to Fourth Post-Minkowskian Order from the Effective Field Theory Approach*, `2106.08276`.

[27] C. Dlapa, G. Kälin, Z. Liu and R. A. Porto, *Conservative Dynamics of Binary Systems at Fourth Post-Minkowskian Order in the Large-eccentricity Expansion*, `2112.11296`.

[28] G. Mogull, J. Plefka and J. Steinhoff, *Classical black hole scattering from a worldline quantum field theory*, *JHEP* **02** (2021) 048 [`2010.02865`].

[29] G. U. Jakobsen, G. Mogull, J. Plefka and J. Steinhoff, *Classical Gravitational Bremsstrahlung from a Worldline Quantum Field Theory*, *Phys. Rev. Lett.* **126** (2021) 201103 [`2101.12688`].

[30] S. Mougiakakos, M. M. Riva and F. Vernizzi, *Gravitational Bremsstrahlung in the post-Minkowskian effective field theory*, *Phys. Rev. D* **104** (2021) 024041 [`2102.08339`].

[31] G. U. Jakobsen, G. Mogull, J. Plefka and J. Steinhoff, *Gravitational Bremsstrahlung and Hidden Supersymmetry of Spinning Bodies*, `2106.10256`.

[32] M. M. Riva and F. Vernizzi, *Radiated momentum in the Post-Minkowskian worldline approach via reverse unitarity*, `2110.10140`.

[33] D. Bini, T. Damour and A. Geralico, *Radiative contributions to gravitational scattering*, *Phys. Rev. D* **104** (2021) 084031 [`2107.08896`].

[34] A. Antonelli, A. Buonanno, J. Steinhoff, M. van de Meent and J. Vines, *Energetics of two-body Hamiltonians in post-Minkowskian gravity*, *Phys. Rev.* **D99** (2019) 104004 [`1901.07102`].

[35] L. Blanchet and T. Damour, *Tail Transported Temporal Correlations in the Dynamics of a Gravitating System*, *Phys. Rev. D* **37** (1988) 1410.

[36] L. Blanchet and G. Schafer, *Gravitational wave tails and binary star systems*, *Class. Quant. Grav.* **10** (1993) 2699.

[37] C. R. Galley and I. Z. Rothstein, *Deriving analytic solutions for compact binary inspirals without recourse to adiabatic approximations*, *Phys. Rev. D* **95** (2017) 104054 [`1609.08268`].

[38] N. T. Maia, C. R. Galley, A. K. Leibovich and R. A. Porto, *Radiation reaction for spinning bodies in effective field theory I: Spin-orbit effects*, *Phys. Rev.* **D96** (2017) 084064 [`1705.07934`].

[39] N. T. Maia, C. R. Galley, A. K. Leibovich and R. A. Porto, *Radiation reaction for spinning bodies in effective field theory II: Spin-spin effects*, *Phys. Rev.* **D96** (2017) 084065 [`1705.07938`].

[40] L. Blanchet, *Gravitational Radiation from Post-Newtonian Sources and Inspiralling Compact Binaries*, *Living Rev.Rel.* **17** (2014) 2 [`1310.1528`].

[41] G. Schäfer and P. Jaranowski, *Hamiltonian formulation of general relativity and post-Newtonian dynamics of compact binaries*, *Living Rev. Rel.* **21** (2018) 7 [`1805.07240`].

[42] T. Damour, P. Jaranowski and G. Schäfer, *Nonlocal-In-Time Action for the Fourth Post-Newtonian Conservative Dynamics of Two-Body Systems*, *Phys. Rev. D* **89** (2014) 064058 [`1401.4548`].

[43] P. Jaranowski and G. Schäfer, *Derivation of local-in-time fourth post-Newtonian ADM Hamiltonian for spinless compact binaries*, *Phys. Rev.* **D92** (2015) 124043 [`1508.01016`].

[44] L. Bernard, L. Blanchet, A. Bohe, G. Faye and S. Marsat, *Dimensional regularization of the IR divergences in the Fokker action of point-particle binaries at the fourth post-Newtonian order*, *Phys. Rev.* **D96** (2017) 104043 [1706.08480].

[45] T. Marchand, L. Bernard, L. Blanchet and G. Faye, *Ambiguity-Free Completion of the Equations of Motion of Compact Binary Systems at the Fourth Post-Newtonian Order*, *Phys. Rev. D* **97** (2018) 044023 [1707.09289].

[46] W. D. Goldberger and I. Z. Rothstein, *An Effective field theory of gravity for extended objects*, *Phys. Rev.* **D73** (2006) 104029 [hep-th/0409156].

[47] W. D. Goldberger, *Les Houches lectures on effective field theories and gravitational radiation*, in *Les Houches Summer School - Session 86*, 1, 2007, hep-ph/0701129.

[48] S. Foffa and R. Sturani, *Effective field theory methods to model compact binaries*, *Class. Quant. Grav.* **31** (2014) 043001 [1309.3474].

[49] I. Rothstein, *Progress in Effective Field Theory Approach to the Binary Inspiral Problem*, *Gen. Rel. Grav.* **46** (2014) 1726.

[50] V. Cardoso and R. A. Porto, *Analytic approximations, perturbation theory, effective field theory methods and their applications*, *Gen. Rel. Grav.* **46** (2014) 1682 [1401.2193].

[51] R. A. Porto, *The effective field theorist's approach to gravitational dynamics*, *Phys. Rept.* **633** (2016) 1 [1601.04914].

[52] C. Galley, A. Leibovich, R. A. Porto and A. Ross, *Tail Effect in Gravitational Radiation Reaction: Time Nonlocality and Renormalization Group Evolution*, *Phys. Rev. D* **93** (2016) 124010 [1511.07379].

[53] R. A. Porto and I. Rothstein, *Apparent Ambiguities in the Post-Newtonian Expansion for Binary Systems*, *Phys. Rev. D* **96** (2017) 024062 [1703.06433].

[54] S. Foffa and R. Sturani, *Dynamics of the gravitational two-body problem at fourth post-Newtonian order and at quadratic order in the Newton constant*, *Phys. Rev. D* **87** (2013) 064011 [1206.7087].

[55] S. Foffa, R. A. Porto, I. Rothstein and R. Sturani, *Conservative dynamics of binary systems to fourth Post-Newtonian order in the EFT approach II: Renormalized Lagrangian*, *Phys. Rev.* **D100** (2019) 024048 [1903.05118].

[56] M. Bianchi and G. Di Russo, *Turning black-holes and D-branes inside out their photon-spheres*, 2110.09579.

[57] G. Cho, B. Pardo and R. A. Porto, *Gravitational radiation from inspiralling compact objects: Spin-spin effects completed at the next-to-leading post-Newtonian order*, *Phys. Rev. D* **104** (2021) 024037 [2103.14612].

[58] D. Bini, T. Damour and A. Geralico, *Sixth post-Newtonian nonlocal-in-time dynamics of binary systems*, *Phys. Rev. D* **102** (2020) 084047 [2007.11239].

[59] J. Blümlein, A. Maier, P. Marquard and G. Schäfer, *The fifth-order post-Newtonian Hamiltonian dynamics of two-body systems from an effective field theory approach*, 2110.13822.

[60] D. Bini, T. Damour and A. Geralico, *Sixth post-Newtonian local-in-time dynamics of binary systems*, *Phys. Rev. D* **102** (2020) 024061 [2004.05407].

[61] O. B. Firsov, *Determination of the forces acting between atoms using the differential effective cross-section for elastic scattering*, *ZhETP* **24** (1953) 279.

[62] J. Vines, *Scattering of two spinning black holes in post-Minkowskian gravity, to all orders in spin, and effective-one-body mappings*, *Class. Quant. Grav.* **35** (2018) 084002 [1709.06016].

[63] G. Cho, S. Dandapat and A. Gopakuma, *Instantaneous third post-Newtonian accurate expressions for the radiated energy and angular momentum during hyperbolic encounters of non-spinning compact objects*, 2111.00818.

[64] W. D. Goldberger and A. Ross, *Gravitational radiative corrections from effective field theory*, *Phys. Rev.* **D81** (2010) 124015 [0912.4254].

[65] R. A. Porto, A. Ross and I. Z. Rothstein, *Spin induced multipole moments for the gravitational wave amplitude from binary inspirals to 2.5 Post-Newtonian order*, *JCAP* **1209** (2012) 028 [1203.2962].

[66] T. Damour, P. Jaranowski and G. Schäfer, *Fourth post-Newtonian effective one-body dynamics*, *Phys. Rev. D* **91** (2015) 084024 [1502.07245].

[67] K. G. Arun, L. Blanchet, B. R. Iyer and M. S. S. Qusailah, *Inspiralling compact binaries in quasi-elliptical orbits: The Complete 3PN energy flux*, *Phys. Rev. D* **77** (2008) 064035 [0711.0302].

[68] E. Herrmann, J. Parra-Martinez, M. S. Ruf and M. Zeng, *Radiative classical gravitational observables at $\mathcal{O}(G^3)$ from scattering amplitudes*, *JHEP* **10** (2021) 148 [2104.03957].

[69] R. A. Porto, *Post-Newtonian Corrections to the Motion of Spinning Bodies in NRGR*, *Phys. Rev. D* **73** (2006) 104031 [gr-qc/0511061].

[70] R. A. Porto, *Next-to-Leading Order Spin-Orbit Effects in the Motion of Inspiralling Compact Binaries*, *Class. Quant. Grav.* **27** (2010) 205001 [1005.5730].

[71] R. A. Porto and I. Z. Rothstein, *Spin(1)Spin(2) Effects in the Motion of Inspiralling Compact Binaries at Third Order in the Post-Newtonian Expansion*, *Phys.Rev.* **D78** (2008) 044012 [0802.0720].

[72] R. A. Porto and I. Z. Rothstein, *Next to Leading Order Spin(1)Spin(1) Effects in the Motion of Inspiralling Compact Binaries*, *Phys.Rev.* **D78** (2008) 044013 [0804.0260].

[73] R. A. Porto, A. Ross and I. Z. Rothstein, *Spin induced multipole moments for the gravitational wave flux from binary inspirals to third Post-Newtonian order*, *JCAP* **1103** (2011) 009 [1007.1312].

[74] G. Cho, R. A. Porto and Z. Yang, *Gravitational radiation from inspiralling compact objects: Spin effects to fourth Post-Newtonian order*, 2201.05138.

[75] J. Blümlein, A. Maier, P. Marquard and G. Schäfer, *The fifth-order post-Newtonian Hamiltonian dynamics of two-body systems from an effective field theory approach: potential contributions*, *Nucl. Phys. B* **965** (2021) 115352 [2010.13672].

[76] S. Foffa and R. Sturani, *Hereditary terms at next-to-leading order in two-body gravitational dynamics*, *Phys. Rev. D* **101** (2020) 064033 [1907.02869].

[77] S. Foffa and R. Sturani, *Near and far zone in two-body dynamics: an effective field theory perspective*, 2103.03190.

[78] G. L. Almeida, S. Foffa and R. Sturani, *Tail contributions to gravitational conservative dynamics*, 2110.14146.

[79] D. Bini, T. Damour and A. Geralico, *Novel approach to binary dynamics: application to the fifth post-Newtonian level*, *Phys. Rev. Lett.* **123** (2019) 231104 [1909.02375].

[80] D. Bini, T. Damour and A. Geralico, *Binary dynamics at the fifth and fifth-and-a-half post-Newtonian orders*, *Phys. Rev. D* **102** (2020) 024062 [2003.11891].

[81] L. Bernard, L. Blanchet, A. Bohe, G. Faye and S. Marsat, *Energy and periastron advance of compact binaries on circular orbits at the fourth post-Newtonian order*, *Phys. Rev.* **D95** (2017) 044026 [1610.07934].

[82] A. Le Tiec, L. Blanchet and B. F. Whiting, *The First Law of Binary Black Hole Mechanics in General Relativity and Post-Newtonian Theory*, *Phys. Rev.* **D85** (2012) 064039 [1111.5378].

[83] L. Blanchet and G. Schaefer, *Higher order gravitational radiation losses in binary systems*, *Mon. Not. Roy. Astron. Soc.* **239** (1989) 845.

[84] C. R. Galley and M. Tiglio, *Radiation reaction and gravitational waves in the effective field theory approach*, *Phys. Rev. D* **79** (2009) 124027.

[85] C. R. Galley, *Classical Mechanics of Nonconservative Systems*, *Phys. Rev. Lett.* **110** (2013) 174301 [1210.2745].

[86] A. Ross, *Multipole expansion at the level of the action*, *Phys. Rev.* **D85** (2012) 125033 [1202.4750].

[87] M. V. S. Saketh, J. Vines, J. Steinhoff and A. Buonanno, *Conservative and radiative dynamics in classical relativistic scattering and bound systems*, 2109.05994.